

Detectable Singularities from Dynamic Radon Data*

B. N. Hahn[†] and E. T. Quinto[‡]

Abstract. In this paper, we use microlocal analysis to understand what X-ray tomographic data acquisition does to singularities of an object which changes during the measuring process. Depending on the motion model, we study which singularities are detected by the measured data. In particular, this analysis shows that, due to the dynamic behavior, not all singularities might be detected, even if the radiation source performs a complete turn around the object. Thus, they cannot be expected to be (stably) visible in any reconstruction. On the other hand, singularities could be added (or masked) as well. To understand this precisely, we provide a characterization of visible and added singularities by analyzing the microlocal properties of the forward and reconstruction operators. We illustrate the characterization using numerical examples.

Key words. dynamic computerized tomography, motion compensation, limited data, microlocal analysis

AMS subject classifications. 44A12, 92C55, 35S30, 58J40

DOI. 10.1137/16M1057917

1. Introduction. The data collection in X-ray computerized tomography (CT) is time-dependent due to the time-dependent rotation of the radiation source around the specimen. A crucial assumption in classical mathematical theory (including modeling, analysis, and derivation of reconstruction algorithms) is that the investigated object does not change during this time period. However, this assumption is violated in many applications, e.g., in medical imaging due to internal organ motion. In this case, the measured data suffer from inconsistencies. In particular, the application of standard reconstruction techniques leads to motion artifacts in the resulting images [42, 43].

Analytic reconstruction methods to compensate for these inconsistencies have been developed for specific types of motion, e.g., affine deformations; see [4, 39, 6]. An inversion formula for the dynamic forward operator in the case of affine motion has been stated in [16], which also serves as a basis for suitable reconstruction methods. A characterization of the null space and the resolution in the semidiscrete setting has been provided in [17]. For general nonaffine deformations, no inversion formula is known so far. In addition to iterative methods (e.g., [3, 21]), approximate inversion formulas exist that accurately reconstruct singularities for fan beam and parallel beam data in the plane [25] and for cone beam data in space [27]. They

*Received by the editors January 22, 2016; accepted for publication (in revised form) April 22, 2016; published electronically August 30, 2016.

<http://www.siam.org/journals/siims/9-3/M105791.html>

[†]Institute of Mathematics, University of Würzburg, D-97074 Würzburg, Germany (bernadette.hahn@mathematik.uni-wuerzburg.de). The research of this author was partially supported by a fellowship of the German Academic Exchange Service (DAAD) under 91536377.

[‡]Department of Mathematics, Tufts University, Medford, MA 02155 (todd.quinto@tufts.edu). The research of this author was partially supported by NSF grant DMS 1311558.

are based on the observation that operators of the form

$$(1) \quad \mathcal{L} = \mathcal{R}_\Gamma^t \mathcal{P} \mathcal{R}_\Gamma f,$$

with forward operator \mathcal{R}_Γ , specially designed pseudodifferential operator \mathcal{P} , and backprojection operator \mathcal{R}_Γ^t (which is, typically, related to the formal dual to \mathcal{R}_Γ), are known to reconstruct singularities of the object. This problem has been further analyzed in an elegant way for the cone beam transform in [26]. In addition, methods developed in the general context of dynamic inverse problems have been successfully applied in CT [41, 18].

Nevertheless, artifacts can still arise in reconstructions, even if the motion is known and the compensation method is exact, as, e.g., in [16]. On the other hand, the dynamic behavior of the object can lead to a limited data problem even if the radiation source rotates completely around the object. This means that some singularities of the object might not be visible in the reconstruction.

To guarantee reliable diagnostics in practice, it is essential to study these limitations carefully. Therefore, our aim is to analyze which singularities are detected by the measured data in the dynamic case and to characterize which of them can be reliably reconstructed or whether they create additional artifacts in the reconstruction process.

In this research, we understand the motion problem using generalized Radon transforms and microlocal analysis. The mathematical model of X-ray tomography with stationary specimen is integration along straight lines [31]. If the object moves during the data acquisition, the measured data can be interpreted as data for a (static) reference object where the integration now takes place along curves rather than straight lines [25, 3, 16]. Microlocal analysis is the rigorous theory of singularities and the study of how Fourier integral operators (FIOs) transform them. Guillemin [13] was the first to make the connection between microlocal analysis and Radon transforms (see also [15, 14]) when he showed that many generalized Radon transforms, R , are FIOs. He showed that, under the microlocal Bolker assumption (see Definition 10 below) and an extra smoothness assumption related to our definition of smoothly periodic (see section 4.1), R^*R is an elliptic pseudodifferential operator. This means that R^*R images all singularities of functions and does not add artifacts. This theorem was exploited in [2] to show that a broad range of Radon transforms on surfaces in \mathbb{R}^n can be “inverted” modulo lower order terms. Greenleaf and Uhlmann [12] and others developed the microlocal analysis of generalized Radon transforms that occur in X-ray CT [36, 29], cone beam CT [7, 23, 27], seismics [5], sonar [37], radar [34], and other applications in tomography.

Microlocal analysis has begun to be used in motion-compensated CT. In [24], Katsevich proved that, under certain completeness conditions on the motion model, the reconstruction operator \mathcal{L} in (1) detects all singularities of the object. This is related to theorems of Beylkin [2] showing that operators like \mathcal{L} are elliptic pseudodifferential operators. In [8] uniqueness is proven for a broad range of Radon transforms on curves. The cone beam CT case is more subtle since artifacts can be added to backprojection reconstructions, even with stationary objects [12, 7]. Katsevich characterized the added artifacts for this case and developed reconstruction algorithms to, at least locally, decrease the effect of those added artifacts. He used this information to develop motion estimation algorithms when the motion model is not known [27].

Motivated by large field of view electron microscopy, [38] presents the microlocal analysis of general curvilinear Radon transforms in \mathbb{R}^3 as well as local reconstruction methods. Analyzing added artifacts for X-ray tomography without motion has been done in [22, 9, 32], and generalizations to other types of tomography have been done in [10, 33, 1].

In this article, we consider general motion models with less restrictive completeness assumptions. To develop our characterization of visible and added singularities, we describe in section 2 the mathematical model for the dynamic case as generalized Radon transform. We also present the mathematical bases of our work, including microlocal analysis. In section 3, we assume that the model is exact and study which object singularities are encoded in the measured data. In section 4 we consider the reconstruction operator in the case of smoothly periodic motion, so the object is in the same state at the end of the scan as at the start. Based on these results, in section 5 we analyze the case when limited data arise, and characterize visible and added singularities in reconstruction methods of filtered backprojection type. Our theoretical results are evaluated on numerical examples in section 6. The more intricate proofs are in the appendix, and we show in Appendix A.5 that our theorems are true even if the weights are arbitrary on the Radon transforms.

2. Mathematical basis. We use the following notation for function spaces. The space of all smooth (i.e., C^∞) functions of compact support is denoted $\mathcal{D}(\mathbb{R}^n)$. A *distribution* is an element of the dual space $\mathcal{D}'(\mathbb{R}^n)$ with the weak-* topology and pointwise convergence (i.e., $u_k \rightarrow u$ in $\mathcal{D}'(\mathbb{R}^n)$ if, for every $f \in \mathcal{D}(\mathbb{R}^n)$, $u_k(f) \rightarrow u(f)$ in \mathbb{R}). Further, $\mathcal{E}(\mathbb{R}^n)$ will denote the set of smooth functions on \mathbb{R}^n ; its dual space, $\mathcal{E}'(\mathbb{R}^n)$, is the set of distributions that have compact support. See [40] for a description of the topologies and properties of these spaces.

A data set in CT can be interpreted as a function (or distribution) with domain $[0, 2\pi] \times \mathbb{R}$. In the static case, the data are 2π -periodic in the first variable, but this does not necessarily hold in the dynamic case since the object does not necessarily return to its initial state at the end of the scanning.

Generally, smooth functions (and hence distributions) are defined on open sets because derivatives will then be well defined. With this in mind, we make the following definition.

Definition 1. *Let g be a function with domain $[0, 2\pi] \times \mathbb{R}^n$ for some $n \in \mathbb{N}$.*

- (i) *We call g smoothly periodic if g extends to a smooth function on $\mathbb{R} \times \mathbb{R}^n$ that is 2π -periodic in the first variable.*
- (ii) *In the nonperiodic case, we call g smooth if, for some $\epsilon > 0$, g extends to a smooth function on $(-\epsilon, 2\pi + \epsilon) \times \mathbb{R}^n$.*

If g is smoothly periodic, then g can be viewed as a smooth function on the unit circle S^1 by identifying 0 and 2π . We define $\mathcal{D}([0, 2\pi] \times \mathbb{R})$ as the set of all smoothly periodic compactly supported functions on $[0, 2\pi] \times \mathbb{R}$, and $\mathcal{D}'([0, 2\pi] \times \mathbb{R})$ is its dual space with the weak-* topology. The set of smoothly periodic functions on $[0, 2\pi] \times \mathbb{R}$, $\mathcal{E}([0, 2\pi] \times \mathbb{R})$ and its dual space $\mathcal{E}'([0, 2\pi] \times \mathbb{R})$, are defined in a similar way. Including the condition of 2π -periodicity in these definitions will simplify the mapping properties of the dynamic forward operator and its dual (see section 4.1).

In general, the object does not return to its initial state at the end of the scanning; i.e., its motion is not 2π -periodic. For this case, we will state our theorems and definitions using

open domains with $\varphi \in (-\epsilon, 2\pi + \epsilon)$ for some $\epsilon > 0$. Finally, distributions can be restricted to open subsets, and microlocal properties that hold on the larger set (e.g., smoothness) hold on the smaller set. So, our theorems are also true when mapping to distributions on $A \times \mathbb{R}$ (i.e., when the data are restricted to $A \times \mathbb{R}$) when $A \subset (-\epsilon, 2\pi + \epsilon)$ is open.

In CT with a stationary specimen, the given data correspond to integrals along straight lines of the distribution $f \in \mathcal{E}'(\mathbb{R}^2)$ describing the X-ray attenuation coefficients of the investigated object. Hence, the mathematical model in the two-dimensional (2D) parallel scanning geometry is given by the Radon line transform

$$(2) \quad \mathcal{R}f(\varphi, s) = \int_{\mathbb{R}^2} f(x) \delta(s - x^T \theta(\varphi)) \, dx,$$

with $s \in \mathbb{R}$, $\varphi \in [0, 2\pi]$, $\theta = \theta(\varphi) = (\cos \varphi, \sin \varphi)^T$, and the δ -distribution. For fixed source and detector position $(\varphi, s) \in [0, 2\pi] \times \mathbb{R}$, the integration takes place over the line

$$(3) \quad l(\varphi, s) = \{x \in \mathbb{R}^2 \mid x^T \theta = s\}.$$

Data acquisition in CT is time-dependent, since the rotation of the radiation source around the object takes a certain amount of time. The source rotation is the only time-dependent part of the scanning procedure since, in modern CT scanners, detector panels are used such that all detector points record simultaneously for each fixed source position. Concerning the mathematical model, this means that a time instance t can be uniquely identified with a source position and vice versa. In terms of the Radon transform, the source position is given by the angle $\varphi \in [0, 2\pi]$, and there is the unique relation to a time instance $t_\varphi \in [0, 2\pi/\phi]$ via

$$\varphi = t_\varphi \phi,$$

with ϕ being the rotation angle of the radiation source. Therefore, throughout the paper, we interpret φ also as a time instance and $[0, 2\pi]$ as a time interval.

2.1. Mathematical model for moving objects in computerized tomography. We now derive the mathematical model for the case when the investigated object changes during the measuring process. A dynamic object is described by a time-dependent function $h : [0, 2\pi] \times \mathbb{R}^2 \rightarrow \mathbb{R}^2$. In the application of CT, $h(\varphi, \cdot) \in \mathcal{E}'(\mathbb{R}^2)$ for a fixed time $\varphi \in [0, 2\pi]$ corresponds to the X-ray attenuation coefficient of the specimen at this particular time instance.

The dynamic behavior of the object is considered to be due to particles which change position in a fixed coordinate system of \mathbb{R}^2 . This physical interpretation of object movement is now incorporated into a mathematical model.

Let $f(x) := h(0, x)$ denote the state of the object at the initial time. We call f a *reference function*. Please note that f is a distribution since $h(0, \cdot) \in \mathcal{E}'(\mathbb{R}^2)$. Further, let $\Gamma : [0, 2\pi] \times \mathbb{R}^2 \rightarrow \mathbb{R}^2$ be a motion model describing the dynamic behavior of the specimen, where $\Gamma(0, x) = x$ and $\Gamma(\varphi, x)$ denotes which particle is at position x at the time instance φ (in other words, $\Gamma(\varphi, x)$ is the location at time $\varphi = 0$ of the particle that is at x at time φ). For fixed $\varphi \in [0, 2\pi]$, we write

$$(4) \quad \Gamma_\varphi x := \Gamma(\varphi, x)$$

to simplify the notation. Using this motion model and the reference function f , we find the state of the object at time instance φ to be

$$(5) \quad h(\varphi, x) = f(\Gamma_\varphi x).$$

Remark 2. In the model (5), each particle keeps its initial intensity over time. However, this means that the mass of the object may no longer be conserved. If the density varies due to the deformation, this can be taken into account by the mathematical model

$$(6) \quad h(\varphi, x) = |\det D\Gamma_\varphi^{-1}x| f(\Gamma_\varphi x).$$

In both cases, the respective FIOs describing the dynamic setting have the same phase function and hence the same canonical relation. Thus, our results provided in this paper hold equivalently for the mass preserving model (6); see also Appendix A.5.

Throughout the paper, we make the following assumptions on the motion model Γ , which we justify by the physical properties of moving objects and imaging systems.

Hypothesis 3. Let $\Gamma : [0, 2\pi] \times \mathbb{R}^2 \rightarrow \mathbb{R}^2$ and let $\Gamma_\varphi x = \Gamma(\varphi, x)$. Assume $\Gamma_0 x = x$. Then Γ is called a motion model and Γ_φ a motion function if there is an $\epsilon > 0$ such that the following hold:

1. Γ extends smoothly to $\Gamma : (-\epsilon, 2\pi + \epsilon) \times \mathbb{R}^2 \rightarrow \mathbb{R}^2$ (so Γ is smooth by Definition 1).
2. For each $\varphi \in (-\epsilon, 2\pi + \epsilon)$, $\Gamma_\varphi : \mathbb{R}^2 \rightarrow \mathbb{R}^2$ is a diffeomorphism.

A motion model is smoothly periodic if it satisfies these conditions for some $\epsilon > 0$ and if Γ is smoothly periodic.

Remark 4.

1. In practical applications in CT, only discrete data are measured. Thus, the object’s motion is ascertained for finitely discrete time instances only, which justifies this (theoretical) assumption of smooth trajectories.

2. Hypothesis 3.2 ensures that two particles cannot move into the same position, and no particle gets lost (or added). The relocation is smooth because Γ is a smooth function.

With the mathematical model of a dynamic object (5), the operator in the dynamic setting is given by

$$(7) \quad \mathcal{R}_\Gamma f(\varphi, s) := \mathcal{R}(f \circ \Gamma_\varphi)(\varphi, s) = \int_{\mathbb{R}^2} f(\Gamma_\varphi x) \delta(s - x^T \theta(\varphi)) dx.$$

Using the change of coordinates $z := \Gamma_\varphi x$, we obtain the representation

$$(8) \quad \mathcal{R}_\Gamma f(\varphi, s) = \int_{\mathbb{R}^2} f(z) |\det D\Gamma_\varphi^{-1}z| \delta(s - (\Gamma_\varphi^{-1}z)^T \theta(\varphi)) dz.$$

Thus, \mathcal{R}_Γ integrates the respective intensity-corrected reference function along the curve

$$(9) \quad C(\varphi, s) = \left\{ x \in \mathbb{R}^2 \mid (\Gamma_\varphi^{-1}x)^T \theta(\varphi) = s \right\}.$$

So, for each (φ, s) , $C(\varphi, s) = \Gamma_\varphi^{-1}(l(\varphi, s))$. Because Γ_φ is a diffeomorphism, each $C(\varphi, s)$ is a smooth simple unbounded curve, and for each φ the curves $s \mapsto C(\varphi, s)$ for $s \in \mathbb{R}$ cover the plane and are mutually disjoint (they foliate the plane).

2.2. Microlocal analysis and Fourier integral operators. In this section we will outline the basic microlocal principles used in the article. We refer to [19, 44, 45, 20, 28] for more details.

The key to understanding singularities and wavefront sets is the relation between smoothness and the Fourier transform: a distribution $f \in \mathcal{E}'(\mathbb{R}^n)$ is smooth if and only if its Fourier transform is rapidly decreasing at infinity. However, to make the definition invariant on manifolds (such as $[0, 2\pi] \times \mathbb{R}$ with 0 and 2π identified), we need to define the wavefront set as a set in the cotangent bundle [44]. So, we will introduce some notation.

Let $x = (x_1, \dots, x_n) \in \mathbb{R}^n$ and $\xi = (\xi_1, \dots, \xi_n) \in \mathbb{R}^n$. Now let h be a smooth scalar function of variables including $x \in \mathbb{R}^2$, and let $G = (g_1, g_2)$ be a function with codomain \mathbb{R}^2 . Then we define

$$\xi dx = \xi_1 dx_1 + \dots + \xi_n dx_n \in T_x^*(\mathbb{R}^n),$$

where $T_x^*(\mathbb{R}^n)$ is the cotangent space at $x \in \mathbb{R}^n$,

$$\partial_x h = \frac{\partial h}{\partial x_1} dx_1 + \frac{\partial h}{\partial x_2} dx_2, \quad D_x h = \left(\frac{\partial h}{\partial x_1}, \frac{\partial h}{\partial x_2} \right), \quad G dx = g_1 dx_1 + g_2 dx_2,$$

and the other derivatives (using D) and differentials (using ∂) are defined in a similar way; for example, $\partial_s h = \frac{\partial h}{\partial s} ds$.

Definition 5. Let $u \in \mathcal{D}'(\mathbb{R}^n)$, and let $(x_0, \xi_0) \in \mathbb{R}^n \times (\mathbb{R}^n \setminus \mathbf{0})$. Then u is smooth at x_0 in direction ξ_0 if there is a cutoff function at x_0 , $\psi \in \mathcal{D}(\mathbb{R}^n)$ (i.e., $\psi(x_0) \neq 0$), and an open cone V containing ξ_0 such that $\mathcal{F}(\psi u)(\xi)$ is rapidly decreasing at infinity for all $\xi \in V$.

On the other hand, if u is not smooth at x_0 in direction ξ_0 , then $(x_0, \xi_0 dx) \in \text{WF}(u)$, the C^∞ wavefront set of u .

We now define the fundamental class of operators on which our analysis is based: FIOs. Note that we define them only for the special case that we use. For other applications, one would use the definition for general spaces in [45, Chapter VI.2] or [19].

Definition 6 (Fourier integral operator (FIO)). Let $\epsilon > 0$. Now let $a(\varphi, s, x, \sigma)$ be a smooth function on $(-\epsilon, 2\pi + \epsilon) \times \mathbb{R} \times \mathbb{R}^2 \times \mathbb{R}$; then a is an amplitude of order k if it satisfies the following condition. For each compact subset K in $(-\epsilon, 2\pi + \epsilon) \times \mathbb{R} \times \mathbb{R}^2$ and $M \in \mathbb{N}$ there exists a positive constant $C_{K,M}$ such that

$$(10) \quad \left| \frac{\partial^{n_1}}{\partial \varphi^{n_1}} \frac{\partial^{n_2}}{\partial s^{n_2}} \frac{\partial^{n_3}}{\partial x_1^{n_3}} \frac{\partial^{n_4}}{\partial x_2^{n_4}} \frac{\partial^m}{\partial \sigma^m} a(\varphi, s, x, \sigma) \right| \leq C_{K,M} (1 + |\sigma|)^{k-m}$$

for $n_1 + n_2 + n_3 + n_4 \leq M$, $m \leq M$, all $(\varphi, s, x) \in K$, and all $\sigma \in \mathbb{R}$.

The real-valued function $\Phi \in C^\infty((-\epsilon, 2\pi + \epsilon) \times \mathbb{R} \times \mathbb{R}^2 \times (\mathbb{R} \setminus \mathbf{0}))$ is called a phase function if Φ is positive homogeneous of degree 1 in σ and both $(\partial_{(\varphi,s)} \Phi, \partial_\sigma \Phi)$ and $(\partial_x \Phi, \partial_\sigma \Phi)$ are nonzero for all $(\varphi, s, x, \sigma) \in (-\epsilon, 2\pi + \epsilon) \times \mathbb{R} \times \mathbb{R}^2 \times \mathbb{R} \setminus \mathbf{0}$. The phase function Φ is called nondegenerate if on the zero-set

$$(11) \quad \Sigma_\Phi = \{(\varphi, s, x, \sigma) \in (-\epsilon, 2\pi + \epsilon) \times \mathbb{R} \times \mathbb{R}^2 \times \mathbb{R} \setminus \mathbf{0} \mid \partial_\sigma \Phi = 0\}$$

one has that $\partial_{\varphi,s,x}(\frac{\partial \Phi}{\partial \sigma}) \neq 0$. In this case, the operator \mathcal{T} defined for $u \in \mathcal{E}'(\mathbb{R}^2)$ by

$$(12) \quad \mathcal{T}u(\varphi, s) = \int e^{i\Phi(\varphi,s,x,\sigma)} a(\varphi, s, x, \sigma) u(x) dx d\sigma$$

is a Fourier integral operator (FIO) of order $k - 1/2$. The canonical relation for \mathcal{T} is

$$(13) \quad C := \{(\varphi, s, \partial_{(\varphi,s)}\Phi(\varphi, s, x, \eta); x, -\partial_x\Phi(\varphi, s, x, \sigma)) \mid (\varphi, s, x, \sigma) \in \Sigma_\Phi\}.$$

Note that since the phase function Φ is nondegenerate, the sets Σ_Φ and C are smooth manifolds. Because of the conditions on a and Φ , $\mathcal{T} : \mathcal{D}(\mathbb{R}^2) \rightarrow \mathcal{E}((-\epsilon, 2\pi + \epsilon) \times \mathbb{R})$ and $\mathcal{T} : \mathcal{E}'(\mathbb{R}^2) \rightarrow \mathcal{D}'((-\epsilon, 2\pi + \epsilon) \times \mathbb{R})$ are continuous in both cases [45]. If the amplitude a and phase function Φ are smoothly periodic, then the conditions in this definition are valid on $[0, 2\pi] \times \mathbb{R} \times \mathbb{R}^2 \times \mathbb{R}$, where 0 and 2π are identified. In this case, $\mathcal{T}u$ is 2π -periodic in φ for all $u \in \mathcal{E}'(\mathbb{R}^2)$.

To state the theorems that form the key to our proofs, we need the following definitions. Let X and Y be sets, and let $B \subset X \times Y$, $C \subset Y \times X$, and $D \subset X$. Then,

$$(14) \quad \begin{aligned} C^t &= \{(x, y) \mid (y, x) \in C\}, \\ C \circ D &= \{y \in Y \mid \exists x \in D, (y, x) \in C\}, \\ B \circ C &= \{(x', x) \in X \times X \mid \exists y \in Y, (x', y) \in B, (y, x) \in C\}. \end{aligned}$$

We will use these expressions to describe what FIOs do to wavefront sets.

Theorem 7 (see [19, Theorem 4.2.1]). *Let \mathcal{T} be an FIO with canonical relation C . Then the formal dual operator, \mathcal{T}^* to \mathcal{T} , is an FIO with canonical relation C^t .*

FIOs transform wavefront sets in precise ways, and our next theorem, a special case of the Hörmander–Sato lemma, is a key to our analysis.

Theorem 8 (see [19, Theorems 2.5.7 and 2.5.14]). *Let \mathcal{T} be an FIO with canonical relation C . Let $f \in \mathcal{E}'(\mathbb{R}^2)$. Then $\text{WF}(\mathcal{T}f) \subset C \circ \text{WF}(f)$.*

To understand the more subtle properties of an FIO, we investigate the mapping properties of the canonical relation C . Let $\Pi_L : C \rightarrow T^*((-\epsilon, 2\pi + \epsilon) \times \mathbb{R}) \setminus \mathbf{0}$ and $\Pi_R : C \rightarrow T^*(\mathbb{R}^2) \setminus \mathbf{0}$ be the natural projections. Then we have the following diagram:

$$(15) \quad \begin{array}{ccc} & C & \\ \Pi_L \swarrow & & \searrow \Pi_R \\ T^*((-\epsilon, 2\pi + \epsilon) \times \mathbb{R}) \setminus \mathbf{0} & & T^*(\mathbb{R}^2) \setminus \mathbf{0} \end{array}$$

First, note that if $B \subset T^*(\mathbb{R}^2)$ and $D \subset T^*((-\epsilon, 2\pi + \epsilon) \times \mathbb{R})$, then

$$(16) \quad C \circ B = \Pi_L(\Pi_R^{-1}(B)), \quad C^t \circ D = \Pi_R(\Pi_L^{-1}(D)).$$

These statements are proven using the definitions of composition and the projections.

The next definition is helpful in determining which singularities are visible.

Definition 9. *The FIO \mathcal{T} in (12) is elliptic of order $m - 1/2$ if its amplitude, a , is of order m and satisfies the following conditions: for each compact set $K \subset (-\epsilon, 2\pi + \epsilon) \times \mathbb{R} \times \mathbb{R}^2$ there are constants $C_K > 0$ and $S_K > 0$ such that for all $(\varphi, s, x) \in K$ and $|\sigma| > S_K$, $|a(\varphi, s, x, \sigma)| \geq C_K(1 + |\sigma|)^m$.*

Ellipticity is defined in a similar way for pseudodifferential operators.

Our next definition is fundamental for our results.

Definition 10. Let \mathcal{T} be an FIO with canonical relation C . Then, \mathcal{T} satisfies the microlocal Bolker assumption if the projection Π_L is an injective immersion.

Note that an immersion is a smooth map with injective differential.

Guillemin [13, 15] called Definition 10 plus some geometric assumptions (including that \mathcal{T} is a Radon transform) the Bolker assumption. His extra assumptions assure that one can compose \mathcal{T}^* and \mathcal{T} and that the composition is an elliptic pseudodifferential operator. This is not true in general without extra assumptions.

Now, we apply these ideas to dynamic tomography.

3. Microlocal analysis of the dynamic forward operator. In this section, we study the microlocal properties of the forward operator \mathcal{R}_Γ in dynamic CT. We show that it is an FIO and provide conditions under which it fulfills the microlocal Bolker assumption. Corollary 16 gives the relationship between singularities of f and those of $\mathcal{R}_\Gamma f$, which is then analyzed in more detail, especially with respect to the importance of the Bolker assumption. Our theorems are true for more general FIO, but the proofs are easier in our special case.

We now introduce some notation and describe its geometric meaning. Here Γ is a motion model that satisfies Hypothesis 3, and let ϵ be as in that hypothesis. For $x \in \mathbb{R}^2$, $\varphi \in (-\epsilon, 2\pi + \epsilon)$ define

$$(17) \quad H(\varphi, x) := (\Gamma_\varphi^{-1}x)^T \theta(\varphi).$$

Then, the integration curve $C(\varphi, s)$ in (9) can be written

$$C(\varphi, s) = \{x \in \mathbb{R}^2 \mid H(\varphi, x) = s\}.$$

Now, define

$$(18) \quad \mathcal{N}(\varphi, x) := \partial_x H(\varphi, x).$$

Our next lemma gives the geometric meaning of this covector.

Lemma 11. Let $(\varphi_0, s_0) \in (-\epsilon, 2\pi + \epsilon) \times \mathbb{R}$, and let x be a point on the integration curve $C(\varphi_0, s_0)$. The vector $D_x H(\varphi_0, x)$ is normal to the curve $C(\varphi_0, s_0)$ at x , and therefore the covector $\mathcal{N}(\varphi_0, x)$ is conormal to this curve at x .

Proof. The curve $C(\varphi_0, s_0)$ is defined by the equation $g(x) := H(\varphi_0, x) - s_0 = 0$. Therefore the gradient in x of g at each $x \in C(\varphi_0, s_0)$, which is $D_x H(\varphi_0, x)$, is normal to this curve at x . So, its dual covector, which is $\mathcal{N}(\varphi_0, x)$, is conormal to $C(\varphi_0, s_0)$ at x (i.e., in the conormal space of $C(\varphi_0, s_0)$ above x). ■

3.1. The canonical relation of \mathcal{R}_Γ . We first prove that the forward operator (8) for the dynamic setting is an elliptic FIO.

Theorem 12. Under Hypothesis 3, the operator \mathcal{R}_Γ is an elliptic FIO of order $-1/2$ with phase function

$$(19) \quad \Phi(\varphi, s, x, \sigma) := \sigma(s - (\Gamma_\varphi^{-1}x)^T \theta(\varphi))$$

and amplitude

$$(20) \quad a(\varphi, s, x, \sigma) := (2\pi)^{-1} |\det D\Gamma_\varphi^{-1}x|,$$

which is elliptic of order zero.

The proof is given in Appendix A.1.

Since \mathcal{R}_Γ is an FIO, we can determine its canonical relation using (13) of Definition 6.

Lemma 13. *Under Hypothesis 3, the canonical relation of \mathcal{R}_Γ is*

$$(21) \quad \mathcal{C}_\Gamma := \left\{ (\varphi, H(\varphi, x), \sigma (ds - \partial_\varphi H(\varphi, x)); x, \sigma \mathcal{N}(\varphi, x)) \mid \varphi \in (-\epsilon, 2\pi + \epsilon), x \in \mathbb{R}^2, \sigma \in \mathbb{R} \setminus \{0\} \right\},$$

where ϵ is as given in Hypothesis 3.

If the motion model is smoothly periodic in φ , then the condition on φ in (21) is replaced by $\varphi \in [0, 2\pi]$, and \mathcal{C}_Γ is still a smooth manifold without boundary when $[0, 2\pi]$ is identified with the unit circle, S^1 .

Proof. According to (13) in Definition 6, the canonical relation of \mathcal{R}_Γ is given by

$$\mathcal{C}_\Gamma := \left\{ (\varphi, s, \partial_{(\varphi, s)}\Phi(\varphi, s, x, \sigma); x, -\partial_x\Phi(\varphi, s, x, \sigma)) \mid (\varphi, s, x, \sigma) \in \Sigma_\Phi \right\},$$

where $\Sigma_\Phi := \{(\varphi, s, x, \sigma) \in (-\epsilon, 2\pi + \epsilon) \times \mathbb{R} \times \mathbb{R}^2 \times \mathbb{R} \setminus 0 \mid \partial_\sigma(\varphi, s, x, \sigma) = 0\}$. Using the representation of the phase function (19) along with (17), $\partial_\sigma\Phi = (s - H(\varphi, x))d\sigma$, and thus $(\varphi, s, x, \sigma) \in \Sigma_\Phi$ if $s = H(\varphi, x)$. The representation of \mathcal{C}_Γ then follows from the representation of the differentials $\partial_{(\varphi, s)}\Phi(\varphi, s, x, \sigma) = -\sigma\partial_\varphi H(\varphi, x) + \sigma ds$ and $\partial_x\Phi(\varphi, s, x, \sigma) = -\sigma\partial_x H(\varphi, x) = -\sigma\mathcal{N}(\varphi, x)$, as noted in the proof of Theorem 12. ■

In the following theorem, we find conditions on the motion model under which \mathcal{R}_Γ satisfies the microlocal Bolker assumption.

Theorem 14. *Assume that the motion model satisfies Hypothesis 3.*

1. *If, for each $\varphi \in (-\epsilon, 2\pi + \epsilon)$, the map*

$$(22) \quad x \mapsto \begin{pmatrix} H(\varphi, x) \\ D_\varphi H(\varphi, x) \end{pmatrix}$$

is one-to-one, then Π_L is injective.

2. *If the motion model fulfills the condition*

$$(23) \quad IC(x, \varphi) := \det \begin{pmatrix} D_x H(\varphi, x) \\ D_x D_\varphi H(\varphi, x) \end{pmatrix} \neq 0$$

for all $x \in \mathbb{R}^2$ and $\varphi \in (-\epsilon, 2\pi + \epsilon)$, then the projection $\Pi_L : \mathcal{C}_\Gamma \rightarrow T^((-\epsilon, 2\pi + \epsilon) \times \mathbb{R}) \setminus 0$ is an immersion.*

Thus, under these two conditions, \mathcal{R}_Γ satisfies the microlocal Bolker assumption (Definition 10).

If the motion is smoothly periodic, then $(-\epsilon, 2\pi + \epsilon)$ can be replaced by $[0, 2\pi]$ in this theorem.

To illustrate the geometric meaning of condition (22) for the motion model, we assume that there exist two points x_1 and x_2 with $H(\varphi, x_1) = H(\varphi, x_2)$ and $D_\varphi H(\varphi, x_1) = D_\varphi H(\varphi, x_2)$ for some $\varphi \in [0, 2\pi]$. The first equality implies that the two points are on the same integration curve; i.e., the data at angle φ cannot distinguish between them. The second equality means that if the angle of view φ changes infinitesimally, also the new curve cannot distinguish the two points because they both stay on the same curve (at least infinitesimally). An example for a motion model not satisfying (22) is any dynamic behavior in which two particles, which are on the same integration curve for a time instance φ , are rotated with the same speed and in the same direction as the radiation source

Condition (23), also referred to as an *immersion condition*, is equivalent to the condition $D_\varphi D_x H(\varphi, x) \notin \text{span} D_x H(\varphi, x)$. The property $\text{IC}(x, \varphi) = 0$ means that, at least infinitesimally at φ_0 , the line normal to the curve $C(\varphi_0, H(\varphi_0, x_0))$ at x_0 is stationary at φ_0 ; i.e., the curves near $C(x_0, H(\varphi_0, x_0))$ are infinitesimally rigid at x_0 (these statements are justified in a related case in [38, Remarks 2 and 5]).

We should remark that the conditions in Theorem 14 are essentially equivalent to the conditions of Theorem 2.1 in [24] for the fan beam case. There is an additional assumption in that theorem that ensures that all singularities are visible in the reconstruction.

Proof of Theorem 14. On the set \mathcal{C}_Γ , we introduce global coordinates (φ, x, σ) by the map

$$(24) \quad \begin{aligned} c : (-\epsilon, 2\pi + \epsilon) \times \mathbb{R}^2 \times \mathbb{R} \setminus 0 &\rightarrow \mathcal{C}_\Gamma, \\ (\varphi, x, \sigma) &\mapsto (\varphi, H(\varphi, x), \sigma(-\partial_\varphi H(\varphi, x) + ds), x, \sigma \mathcal{N}(\varphi, x)). \end{aligned}$$

In these coordinates, the projection Π_L is given by

$$(25) \quad \Pi_L(\varphi, x, \sigma) = (\varphi, H(\varphi, x), -\sigma \partial_\varphi H(\varphi, x) + \sigma ds).$$

Using the representation (25) of Π_L , one sees that Π_L is injective if for each $\varphi \in (-\epsilon, 2\pi + \epsilon)$, the map in (22) is injective.

The map Π_L is an immersion if its differential has constant rank 4. A calculation shows that this is equivalent to

$$\det \begin{pmatrix} D_{x_1} H(\varphi, x) & D_{x_2} H(\varphi, x) \\ -\sigma D_{x_1} D_\varphi H(\varphi, x) & -\sigma D_{x_2} D_\varphi H(\varphi, x) \end{pmatrix} \neq 0,$$

which is (23). ■

The importance of this Bolker assumption for the detection of object singularities in dynamic Radon data is discussed in the next section.

3.2. Visible singularities. Now, we algebraically and geometrically classify singularities of functions that appear in the data.

Theorem 15. *Assume that the motion model, Γ , satisfies Hypothesis 3. Let $f \in \mathcal{E}'(\mathbb{R}^2)$. Then*

$$(26) \quad \text{WF}(\mathcal{R}_\Gamma f) \subset \mathcal{C}_\Gamma \circ \text{WF}(f).$$

Now, assume also that \mathcal{R}_Γ satisfies the microlocal Bolker assumption. Then,

$$(27) \quad \text{WF}(\mathcal{R}_\Gamma f) = \mathcal{C}_\Gamma \circ \text{WF}(f).$$

We will prove this theorem in Appendix A.2.

The explicit correspondence between object and data singularities is given in the following corollary.

Corollary 16. *Let $f \in \mathcal{E}'(\mathbb{R}^2)$, and let Γ be a motion model satisfying Hypothesis 3. Let $(\varphi_0, s_0) \in (-\epsilon, 2\pi + \epsilon) \times \mathbb{R}$, $\sigma \neq 0$, $\beta \in \mathbb{R}$.*

If $(\varphi_0, s_0; \sigma(ds - \beta d\varphi)) \in \text{WF}(\mathcal{R}_\Gamma f)$, then there is an $x_0 \in C(\varphi_0, s_0)$ such that

$$(x_0, \sigma\mathcal{N}(\varphi_0, x_0)) \in \text{WF}(f),$$

where $C(\varphi_0, s_0)$ is the integration curve given by (9) and \mathcal{N} is given by (18).

Assume in addition that \mathcal{R}_Γ satisfies the microlocal Bolker assumption. For $\varphi_0 \in (-\epsilon, 2\pi + \epsilon)$,

$$(28) \quad \begin{aligned} &(\varphi_0, s_0; \sigma(ds - \beta d\varphi)) \in \text{WF}(\mathcal{R}_\Gamma f) \\ &\text{if and only if there is an } x_0 \in C(\varphi_0, s_0) \text{ such that} \\ &\partial_\varphi H((\varphi_0, x_0) = \beta \text{ and } (x_0, \sigma\mathcal{N}(\varphi_0, x_0)) \in \text{WF}(f). \end{aligned}$$

Furthermore, if such a point x_0 exists, then it is unique.

The proof follows immediately from Theorem 15 and the expression (21) for the canonical relation \mathcal{C}_Γ . In particular, the first statement follows from (26), and the equivalence (28) follows from the injectivity assumption in Definition 10 as well as (24), (25), and (27).

For $B \subset (-\epsilon, 2\pi + \epsilon) \times \mathbb{R}$ define

$$(29) \quad T_B^*((-\epsilon, 2\pi + \epsilon) \times \mathbb{R}) = \left\{ (\varphi, s, \eta) \mid (\varphi, s) \in B, \eta \in T_{(\varphi, s)}^*((-\epsilon, 2\pi + \epsilon) \times \mathbb{R}) \right\}.$$

We now define what we mean for a singularity of f to be visible in the data.

Definition 17. *Let $A \subset (-\epsilon, 2\pi + \epsilon)$, and let Γ be a motion model satisfying Hypothesis 3. Assume that the associated Radon transform, \mathcal{R}_Γ , satisfies the microlocal Bolker assumption. Let $f \in \mathcal{E}'(\mathbb{R}^2)$, and let $(x_0, \xi_0) \in \text{WF}(f)$. Then we will call (x_0, ξ_0) a visible singularity from data above A (or visible in the data) if ξ_0 has the representation*

$$(30) \quad \xi_0 = \sigma\mathcal{N}(\varphi_0, x_0)$$

for some $\sigma \neq 0$ and $\varphi_0 \in A$.

We call

$$(31) \quad \mathcal{V}_A = \{ (x, \sigma\mathcal{N}(\varphi, x)) \mid x \in \mathbb{R}^2, \varphi \in A, \sigma \neq 0 \}$$

the set of all potentially visible singularities from data above A . Covectors in

$$\mathcal{I}_A = (T^*(\mathbb{R}^2) \setminus \mathbf{0}) \setminus \mathcal{V}_{\text{cl}(A)}$$

will be called invisible singularities from A .

Using (16), it follows that

$$(32) \quad \mathcal{V}_A = \mathcal{C}_\Gamma^t \circ T_{A \times \mathbb{R}}^*((-\epsilon, 2\pi + \epsilon) \times \mathbb{R}) = \Pi_R \left(\Pi_L^{-1} \left(T_{A \times \mathbb{R}}^*((-\epsilon, 2\pi + \epsilon) \times \mathbb{R}) \right) \right).$$

Remark 18. We now use Corollary 16 to justify the definition. If the motion model satisfies Hypothesis 3, and if \mathcal{R}_Γ satisfies the microlocal Bolker assumption, then a singularity $(x, \xi) \in \text{WF}(f)$ causes a singularity from the data $\mathcal{R}_\Gamma f$ above the open set A (i.e., in $T_{A \times \mathbb{R}}^*((-\epsilon, 2\pi + \epsilon) \times \mathbb{R})$) if and only if (x, ξ) is in \mathcal{V}_A . The singularities of f that are in \mathcal{I}_A are smoothed by \mathcal{R}_Γ . Note that the singularities of f in $\mathcal{V}_{\text{bd}(A)}$ are problematic because they are in directions that can be detectable or masked.

The geometric meaning of the visible singularities is described in our next result.

Corollary 19. *Let the motion model fulfill the microlocal Bolker assumption. The dynamic operator \mathcal{R}_Γ detects a singularity of f at a point x_0 in direction ξ_0 if and only if there is an integration curve passing through x_0 with ξ_0 conormal to the curve at x_0 (i.e., the curve has tangent line at this point that is normal to ξ_0).*

Proof. Let $s_0 = H(\varphi_0, x_0)$. Corollary 16 shows that, under the microlocal Bolker assumption, a singularity of f at (x_0, ξ_0) is detectable if and only if $\xi_0 = \sigma \mathcal{N}(\varphi_0, x_0)$ for some $\sigma \neq 0$. Furthermore, Lemma 11 establishes that for each $(\varphi, s) \in (-\epsilon, 2\pi + \epsilon) \times \mathbb{R}$ and each $x \in C(\varphi, s)$ the covector $\mathcal{N}(\varphi, x)$ is conormal to $C(\varphi, s)$ at x . Thus a singularity of f at (x_0, ξ_0) is detectable if and only if ξ_0 is conormal to $C(\varphi_0, s_0)$ at x_0 . ■

Remark 20. In general, each data singularity at a point in data space, (φ_0, s_0) , stems from an object singularity at a point $x_0 \in C(\varphi_0, s_0)$ with direction ξ_0 , where ξ_0 is perpendicular to the curve $C(\varphi_0, s_0)$ at x_0 . However, in case the microlocal Bolker assumption is not fulfilled by the motion model, two object singularities could cancel in the data and thus not lead to a corresponding data singularity.

In contrast, under the microlocal Bolker assumption, every singularity in the data comes from a singularity in the object. Note that Example 22 shows that not all singularities of the object necessarily show up in the data.

Another way to understand detectable singularities is the following. $(x_0, \xi_0) \in \mathcal{V}_A$ if there is some $\sigma \neq 0$ and $\varphi_0 \in A$ such that $\xi_0 \in \text{Range}(\mu_{x_0})$, where μ_{x_0} is the map

$$(33) \quad \mu_{x_0}(\sigma, \varphi_0) = \sigma \mathcal{N}(\varphi_0, x_0)$$

for $(\sigma, \varphi_0) \in (\mathbb{R} \setminus \mathbf{0}) \times A$ (see (30)). If this map μ_{x_0} is not injective, the object singularity x_0 can cause multiple singularities in the data, resulting in redundant data, as illustrated by our next example.

Example 21. *Let the dynamic behavior of f be given by the rotation $\Gamma_\varphi x = A_\varphi x$ with rotation matrix*

$$A_\varphi = \begin{pmatrix} \cos \varphi & -\sin \varphi \\ \sin \varphi & \cos \varphi \end{pmatrix}.$$

This describes an object which rotates in the direction opposite to the motion of the radiation source, with the same rotational speed. In particular, it holds that $\Gamma_\varphi = \Gamma_{\varphi+2\pi}$ for $\varphi \in [0, 2\pi]$, so this is a smoothly periodic motion model. Since A_φ is a unitary matrix for all $\varphi \in [0, 2\pi]$, we have

$$H(\varphi, x) = (A_\varphi^{-1}x)^T \theta(\varphi) = x^T A_\varphi \theta(\varphi) = x^T \theta(2\varphi).$$

By a calculation using (23), $IC(x, \varphi) = 2 \cos^2(2\varphi) + 2 \sin^2(2\varphi) = 2$, and the map

$$x \mapsto \begin{pmatrix} x^T \theta(2\varphi) \\ 2 x^T \theta(2\varphi)^\perp \end{pmatrix}$$

is one-to-one since the matrix $(\theta(2\varphi), \theta(2\varphi)^\perp)^T$ is nonsingular. Thus, the dynamic operator \mathcal{R}_Γ satisfies the microlocal Bolker assumption, and $\text{WF}(\mathcal{R}_\Gamma f) = \mathcal{C}_\Gamma \circ \text{WF}(f)$.

Now, let $(x_0, \xi_0 dx) \in \text{WF}(f)$ with $\xi_0 := \theta(\pi)$. Since $\mathcal{N}(\frac{\pi}{2}, x_0) = \mathcal{N}(\frac{3\pi}{2}, x_0) = \xi_0$, this one singularity in object space causes two singularities in data space:

$$\begin{aligned} \left(\frac{\pi}{2}, H \left(\frac{\pi}{2}, x_0 \right), \sigma ds - \sigma x^T \theta^\perp(\pi) d\varphi \right) &\in \text{WF}(\mathcal{R}_\Gamma) \quad \text{and} \\ \left(\frac{3\pi}{2}, H \left(\frac{3\pi}{2}, x_0 \right), \sigma ds - \sigma x^T \theta^\perp(\pi) d\varphi \right) &\in \text{WF}(\mathcal{R}_\Gamma). \end{aligned}$$

This is according to the fact that the projection $\Pi_R : \mathcal{C}_\Gamma \rightarrow T^*(\mathbb{R}^2) \setminus 0$ is not injective due to the motion-introduced data redundancy.

In [27], a motion estimation procedure based on redundant data singularities was proposed: if multiple edges are seen twice and the motion model is known incorrectly, the reconstructed image will appear cluttered, which can then be used to iteratively determine optimal motion parameters.

If the map μ_{x_0} in (33) is surjective for all $x_0 \in \mathbb{R}^2$ and the motion model satisfies the microlocal Bolker assumption, then all singularities in all directions are gathered in the measured data, and we speak of complete data. In the static case, this occurs when the radiation source rotates around the object in a complete circle (see, e.g., [35]). If μ_{x_0} is not surjective, then the point x_0 is only probed by curves from a limited angular range. The following example illustrates that the dynamic behavior of the object can lead to incomplete data, even if the source rotates through a complete circle.

Example 22. We consider the rotational movement $\Gamma_\varphi x = A_\varphi x$ with

$$A_\varphi = \begin{pmatrix} \cos(\frac{2}{3}\varphi) & \sin(\frac{2}{3}\varphi) \\ -\sin(\frac{2}{3}\varphi) & \cos(\frac{2}{3}\varphi) \end{pmatrix}.$$

In this setting, the object rotates in the same direction as the radiation source with half of its rotation speed. In particular, this is a nonperiodic motion model, and

$$H(\varphi, x) = x^T A_\varphi \theta(\varphi) = x^T \begin{pmatrix} \cos(\frac{\varphi}{3}) \\ \sin(\frac{\varphi}{3}) \end{pmatrix}.$$

One shows that the injectivity condition (22) is fulfilled in the same way as in Example 21. Computing the derivatives, we obtain $IC(x, \varphi) = \frac{1}{3} \cos^2(\frac{\varphi}{3}) + \frac{1}{3} \sin^2(\frac{\varphi}{3}) = \frac{1}{3}$. So, the microlocal Bolker assumption holds.

Now, assume $(x_0, \xi_0 dx) \in \text{WF}(f)$ with $\xi_0 = \theta(\frac{5\pi}{6})$. According to Theorem 15, a corresponding singularity is seen in the data if there exists an angle $\varphi_0 \in [0, 2\pi]$ with $\xi_0 = A_{\varphi_0} \theta(\varphi_0) = \theta(\frac{\varphi_0}{3})$ or $\xi_0 = -A_{\varphi_0} \theta(\varphi_0) = \theta(\frac{-\varphi_0}{3})$. Since $\frac{\varphi_0}{3} \in [0, \frac{2}{3}\pi]$ for all $\varphi_0 \in [0, 2\pi]$, an angle φ_0 with the required property does not exist. Hence, the singularity $(x_0, \xi_0 dx) \in \text{WF}(f)$ cannot be seen in the data.

4. The dynamic reconstruction operator for smoothly periodic motion. In this section, we prove the main theorem for smoothly periodic motion. Basically, under our assumptions, the reconstruction operator is well-behaved and reconstructs all singularities of the object without introducing new artifacts. First, we define the backprojection operator.

4.1. Backprojection for smoothly periodic motion. In general, we denote the backprojection operator by \mathcal{R}_Γ^t and define it as

$$(34) \quad \mathcal{R}_\Gamma^t g(x) = \int_{\varphi \in [0, 2\pi]} |\det D\Gamma_\varphi^{-1}x| g(\varphi, (\Gamma_\varphi^{-1}x)^T \theta(\varphi)) \, d\varphi.$$

Note that, for smoothly periodic motion, this backprojection operator is the formal dual, \mathcal{R}_Γ^* , to \mathcal{R}_Γ for $g \in \mathcal{E}([0, 2\pi] \times \mathbb{R})$. A generalization to arbitrary weights is explained in Appendix A.5.

Proposition 23. *If the motion model Γ_φ is smoothly periodic, then the backprojection operator, \mathcal{R}_Γ^t , can be composed with \mathcal{R}_Γ for $f \in \mathcal{E}'(\mathbb{R}^2)$ and, if \mathcal{P} is a pseudodifferential operator, then the reconstruction operator $\mathcal{L} = \mathcal{R}_\Gamma^t \mathcal{P} \mathcal{R}_\Gamma$ is defined and continuous on domain $\mathcal{E}'(\mathbb{R}^2)$.*

Proof. The proof will now be outlined. First, we show that when $f \in \mathcal{D}(\mathbb{R}^2)$, $\mathcal{R}_\Gamma f \in \mathcal{D}([0, 2\pi] \times \mathbb{R})$. By the smoothness assumptions on Γ_φ , the integrals over $C(\varphi, s)$ vary smoothly in each variable, and because Γ_φ is 2π -periodic, the curves are 2π -periodic (i.e., $C(\varphi + 2\pi, s) = C(\varphi, s)$). Thus, the integrals $\mathcal{R}_\Gamma f(\varphi, s)$ are smooth and 2π -periodic because each $f \in \mathcal{D}(\mathbb{R}^2)$ has fixed compact support and Γ_φ is 2π -periodic. Now, to show that \mathcal{R}_Γ is continuous, one considers the seminorms on $\mathcal{D}([0, 2\pi] \times \mathbb{R})$ (see [40, Part II, section 6.3]). So, assume $f_k \rightarrow f$ in $\mathcal{D}(\mathbb{R}^2)$; this means that the sequence (f_k) and all derivatives converge uniformly to those of f , and the f_k and f are all supported in a fixed compact set $K \subset \mathbb{R}^2$. By the continuity of Γ_φ and compactness of $[0, 2\pi]$, there is an $R > 0$ such that $C(\varphi, s) \cap K = \emptyset$ for $|s| > R$, so $\mathcal{R}_\Gamma f_k$ and $\mathcal{R}_\Gamma f$ are supported in $[0, 2\pi] \times [-R, R]$. Finally, one uses Lebesgue’s dominated convergence theorem and properties of derivatives of integrals to show that $\mathcal{R}_\Gamma f_k$ and all derivatives in φ, s converge uniformly to those of $\mathcal{R}_\Gamma f$ and are all supported in a fixed compact set in $[0, 2\pi] \times \mathbb{R}$. Since \mathcal{R}_Γ^t is the formal dual to \mathcal{R}_Γ in the smoothly periodic case, an analogous proof shows that $\mathcal{R}_\Gamma^t : \mathcal{E}([0, 2\pi] \times \mathbb{R}) \rightarrow \mathcal{E}(\mathbb{R}^2)$ is continuous.

By duality, if the motion is smoothly periodic, then $\mathcal{R}_\Gamma : \mathcal{E}'(\mathbb{R}^2) \rightarrow \mathcal{E}'([0, 2\pi] \times \mathbb{R})$ and $\mathcal{R}_\Gamma^t : \mathcal{D}'([0, 2\pi] \times \mathbb{R}) \rightarrow \mathcal{D}'(\mathbb{R}^2)$ are both weakly continuous. Since $\mathcal{P} : \mathcal{E}'([0, 2\pi] \times \mathbb{R}) \rightarrow \mathcal{D}'([0, 2\pi] \times \mathbb{R})$ is also continuous, \mathcal{L} is weakly continuous. ■

4.2. The main theorem for smoothly periodic motion. Our main theorem for this case gives conditions under which our reconstruction operator images all singularities and adds no artifacts. It is a parallel beam analogue of the fan beam result of Katsevich [24, Theorem 2.1]. However, in that article, the backprojection operator has a different measure; our proof would still be valid in this case (see Appendix A.5). The same distinctions apply to [2] and the proof outline in the last section of [29] for generalized Radon transforms. Furthermore, because of their goals, those authors consider only a few special filters, \mathcal{P} .

Theorem 24. *Assume that the motion model is smoothly periodic and that \mathcal{R}_Γ satisfies the microlocal Bolker assumption. Let $\mathcal{L} = \mathcal{R}_\Gamma^t \mathcal{P} \mathcal{R}_\Gamma$, where \mathcal{P} is an elliptic pseudodifferential*

operator with everywhere positive symbol. Then, \mathcal{L} is an elliptic pseudodifferential operator. Therefore, for any $f \in \mathcal{E}'(\mathbb{R}^2)$,

$$(35) \quad \text{WF}(\mathcal{L}F) = \text{WF}(f).$$

The proof of Theorem 24 will be given in Appendix A.3.

Remark 25. We highlight several implications of the theorem and its proof.

By (35), all singularities are *visible in the reconstruction* if the motion is smoothly periodic and satisfies the microlocal Bolker assumption.

Furthermore, in Remark 29, we prove that \mathcal{L} is elliptic as long as the pseudodifferential operator \mathcal{P} is positive on $\Pi_L(C)$. The standard Lambda tomography filter $\mathcal{P} = -d^2/ds^2$ and the standard filtered backprojection operator $\mathcal{P} = \sqrt{-d^2/ds^2}$ both satisfy this condition, even though their symbols are not elliptic on $T^*([0, 2\pi] \times \mathbb{R})$.

Finally, the positivity condition can be further relaxed, and this will be explained in Remark 29.

5. Nonperiodic motion and added artifacts. If the motion model is smoothly periodic and satisfies the microlocal Bolker assumption, then all singularities are visible in the data and in the reconstruction. That is, $\mathcal{L} = \mathcal{R}_\Gamma^t \mathcal{P} \mathcal{R}_\Gamma$ reconstructs all singularities if \mathcal{P} is elliptic with positive symbol (see Theorem 24 and Remark 25). However, in smoothly periodic motion, the investigated object is in the same state at the beginning and end of the data acquisition. Thus, in applications, this condition will in general not be met.

In this section, we therefore study what can be said for nonperiodic motion models under the microlocal Bolker assumption. We assume that the model satisfies Hypothesis 3, so the motion model is defined on $(-\epsilon, 2\pi + \epsilon) \times \mathbb{R}$ for some $\epsilon > 0$. However, in practice, the data are taken only on $[0, 2\pi] \times \mathbb{R}$. Note that the microlocal analysis developed in section 3 is valid on an open interval and, for nonperiodic motion, data are given on $[0, 2\pi] \times \mathbb{R}$. This creates problems that we will now analyze.

5.1. The forward and backprojection operators for nonperiodic motion. Since the data are given on $[0, 2\pi] \times \mathbb{R}$, the forward operator must be restricted, so \mathcal{R}_Γ must be multiplied by the characteristic function of $[0, 2\pi] \times \mathbb{R}$ to restrict to the data set. Therefore, the restricted forward operator is

$$(36) \quad \mathcal{R}_{\Gamma, [0, 2\pi]} := \chi_{[0, 2\pi] \times \mathbb{R}} \mathcal{R}_\Gamma.$$

For convenience in the proof, the backprojection operator will use the formal dual to \mathcal{R}_Γ on $(-\epsilon, 2\pi + \epsilon) \times \mathbb{R}$ rather than \mathcal{R}_Γ^t . One can show for integrable functions g that the formal dual to \mathcal{R}_Γ is defined by

$$(37) \quad \mathcal{R}_\Gamma^* g(x) = \int_{(-\epsilon, 2\pi + \epsilon)} |\det D\Gamma_\varphi^{-1} x| g(\varphi, (\Gamma_\varphi^{-1} x)^T \theta(\varphi)) d\varphi.$$

Since \mathcal{R}_Γ^* does not have domain $\mathcal{D}'((-\epsilon, 2\pi + \epsilon) \times \mathbb{R})$, we multiply by a cutoff function. Let $\psi : (-\epsilon, 2\pi + \epsilon) \rightarrow \mathbb{R}$ be equal to one on $[0, 2\pi] \times \mathbb{R}$ and be supported in $(-\epsilon, 2\pi + \epsilon)$. We let

$$(38) \quad \mathcal{R}_{\Gamma, \psi}^t g = \mathcal{R}_\Gamma^* (\psi g).$$

Proposition 31 shows that this restricted dual is defined for $g \in \mathcal{D}'((-\epsilon, 2\pi + \epsilon) \times \mathbb{R})$.

The restricted reconstruction operator is defined as

$$(39) \quad \mathcal{L}_{[0,2\pi]} = \mathcal{R}_{\Gamma, \psi}^t \mathcal{P} \mathcal{R}_{\Gamma, [0,2\pi]},$$

where \mathcal{P} is a pseudodifferential operator in data space. In the course of the proof of Theorem 26 we will prove that these operators are defined for distributions and can be composed (see Proposition 31). Furthermore, note that our theorems are trivially valid on any subinterval of $[0, 2\pi]$ by scaling.

5.2. Characterization of artifacts for the reconstruction operator with nonperiodic motion. In the following, we characterize the propagation of singularities under reconstruction in the case of a nonperiodic motion model.

Let $A \subset (-\epsilon, 2\pi + \epsilon)$; then, for $f \in \mathcal{E}'(\mathbb{R}^2)$, we define

$$(40) \quad \text{WF}_A(f) := \text{WF}(f) \cap \mathcal{V}_A,$$

where \mathcal{V}_A is defined in (31). When A is open and \mathcal{R}_Γ satisfies the microlocal Bolker assumption, then Remark 18 justifies why $\text{WF}_A(f)$ is the set of singularities of f that are visible in data of $\mathcal{R}_\Gamma f$ over $A \times \mathbb{R}$. However, it is more subtle to characterize which singularities of f are visible in the reconstruction, which we now do.

Theorem 26. *Let $f \in \mathcal{E}'(\mathbb{R}^2)$, \mathcal{P} be a pseudodifferential operator, and $\mathcal{L}_{[0,2\pi]}$ be given by (39). Then,*

$$\text{WF}(\mathcal{L}_{[0,2\pi]} f) \subset \text{WF}_{[0,2\pi]}(f) \cup \mathcal{A}(f),$$

where

$$(41) \quad \mathcal{A}(f) := \{(\tilde{x}, \sigma \mathcal{N}(\tilde{x}, \varphi)) : \varphi \in \{0, 2\pi\}, s \in \mathbb{R}, \tilde{x} \in C(\varphi, s), \sigma \neq 0, \\ \text{and } \exists x \in C(\varphi, s), (x, \sigma(\mathcal{N}(\varphi, x))) \in \text{WF}(f)\}$$

denotes the set of possible added artifacts.

Remark 27. This theorem shows that only singularities $(x, \xi) \in \text{WF}(f)$ with directions in the visible angular range can be reconstructed from dynamic data. Singularities of f outside of $\mathcal{V}_{[0,2\pi]}$ are smoothed.

Additionally, if f has a singularity at a covector $(x, \sigma \mathcal{N}(\varphi_0, x))$, where $\varphi_0 \in \{0, 2\pi\}$, then that singularity can generate artifacts all along the curve $C(\varphi_0, H(\varphi_0, x))$. These covectors are in the set

$$\mathcal{C}(\varphi_0, x, \sigma) = \{(\tilde{x}, \sigma \mathcal{N}(\varphi_0, \tilde{x})) \mid \tilde{x} \in C(\varphi_0, H(\varphi_0, x))\}.$$

Note that the covector $\mathcal{N}(\varphi_0, \tilde{x})$ is conormal to the curve $C(\varphi_0, H(\varphi_0, x))$ at \tilde{x} by Lemma 11.

Furthermore, the set $\mathcal{A}(f)$ is the union of the $\mathcal{C}(\varphi_0, x, \sigma)$ for

$$\varphi_0 \in \{0, 2\pi\}, \quad (x, \sigma \mathcal{N}(\varphi_0, x)) \in \text{WF}(f).$$

Under an ellipticity condition on \mathcal{P} , we will also have a lower bound on the singularities of f that are visible in the reconstruction $\mathcal{L}_{[0,2\pi]} f$.

Theorem 28. *Let \mathcal{R}_Γ be a motion model satisfying the microlocal Bolker assumption. Assume that \mathcal{P} is an elliptic pseudodifferential operator. Finally, assume the uniqueness condition*

$$(42) \quad \forall(x, \xi) \in T^*(\mathbb{R}^2), \text{ there is at most one } (\varphi, s) \in (-\epsilon, 2\pi + \epsilon) \times \mathbb{R} \text{ with} \\ x \in C(\varphi, s) \text{ and } \xi \text{ conormal to } C(\varphi, s) \text{ at } x$$

holds. Then,

$$(43) \quad \text{WF}_{(0,2\pi)}(f) = \text{WF}_{(0,2\pi)}(\mathcal{L}_{[0,2\pi]}f),$$

where $\text{WF}_{(0,2\pi)}$ is defined in (40).

Descriptively, condition (42) means that the motion does not produce redundant integration curves (i.e., no two curves are ever tangent to each other). Under the assumptions of this theorem, singularities of f in $\mathcal{V}_{(0,2\pi)}$ will be visible in the reconstruction. In general, this result does not mean *all* singularities of f can be recovered; in the limited data case, such as in Example 22, some singularities will likely be invisible from the data.

Theorem 28 is valid under some weaker assumptions, but the statements are more technical (similar to the description in Remark 29). The biggest obstacle to weakening the uniqueness assumption (42) occurs when a singularity at (x, ξ) is conormal to a curve $C(\varphi_0, s_0)$ for $\varphi_0 \in (0, 2\pi)$ and conormal to curves at ends of the angular range: $C(0, s_1)$ or $C(2\pi, s_2)$. Then, added artifacts along $C(0, s_1)$ or $C(2\pi, s_2)$ could cancel a real singularity at (x, ξ) . Ellipticity theorems with more general assumptions than (42) are given for the hyperplane transform in [11, Theorem 5.4], and similar assumptions could be given here.

5.3. An artifact reduction strategy. For motion that is not smoothly periodic, there is another way to handle the limited data for φ in $[0, 2\pi]$ rather than multiplying by a sharp cutoff, $\chi_{[0,2\pi] \times \mathbb{R}}$. One can make \mathcal{R}_Γ and \mathcal{R}_Γ^t 2π -periodic by multiplying by a smooth cutoff function, ϕ , in φ that has compact support in $(0, 2\pi)$ and is equal to one on most of this interval. In this case, the smoothed reconstruction operator would be

$$(44) \quad \mathcal{L}_\phi(f) = (\mathcal{R}_\Gamma^t \phi) \mathcal{P}(\phi \mathcal{R}_\Gamma f),$$

and, for $f \in \mathcal{D}(\mathbb{R}^2)$, $\phi \mathcal{R}_\Gamma f$ is smooth and 2π -periodic so it is in $\mathcal{D}([0, 2\pi] \times \mathbb{R})$. Then, these operators can be composed and are continuous on distributions, and the proof is essentially the same as the proof of Proposition 23.

Under the microlocal Bolker assumption, $(\mathcal{R}_\Gamma^t \phi) (\mathcal{P}(\phi \mathcal{R}_\Gamma))$ is a standard pseudodifferential operator. The proof is essentially the same as in the smoothly periodic case because $\phi \mathcal{R}_\Gamma$ and its formal adjoint, $\mathcal{R}_\Gamma^* \phi = \mathcal{R}_\Gamma^t \phi$, are FIO, satisfying the microlocal Bolker assumption.

It is important to point out that this reconstruction operator is not necessarily elliptic everywhere, even though it is a standard pseudodifferential operator. Furthermore, not only the added artifacts will be smoothed out; visible singularities near $\mathcal{A}(f)$ (i.e., for covectors $(x, \eta(\varphi, x))$ for φ near 0 or 2π) will be attenuated as well, because the cutoff ϕ is zero near 0 and 2π .

This idea has been used in X-ray tomography without motion in [9, 11], and generalizations to nonsmooth cutoffs are in [22]. The analogous idea is used in [24] for motion compensated CT in the fan-beam case.

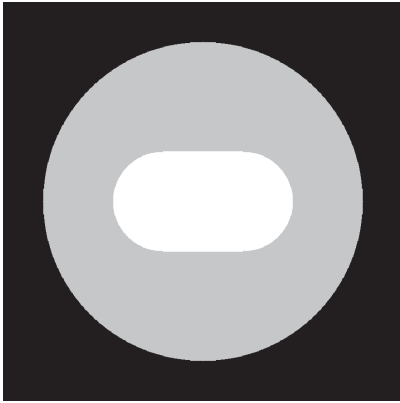


Figure 1. Object at time instance $\varphi = 0$ (reference object).

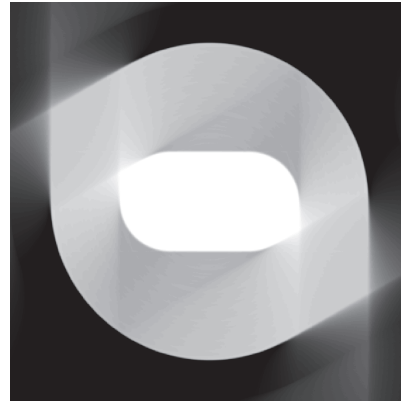


Figure 2. Reconstruction incorporating the exact motion functions.

6. Numerical examples. In this section, we use our theoretical results to analyze the information content in the measured data using numerical examples. First, we consider a specimen which performs a rotational movement during the data acquisition, in addition to the rotation of the radiation source, where $\Gamma_{\varphi}x = A_{\varphi}x$, $x \in \mathbb{R}^2$, $\varphi \in [0, 2\pi]$ with the unitary matrix from Example 22:

$$A_{\varphi} := \begin{pmatrix} \cos(\frac{2}{3}\varphi) & \sin(\frac{2}{3}\varphi) \\ -\sin(\frac{2}{3}\varphi) & \cos(\frac{2}{3}\varphi) \end{pmatrix}, \quad \varphi \in [0, 2\pi].$$

Note that this rotation is not 2π -periodic.

The initial state, i.e., the reference function f , of our specimen is displayed in Figure 1. The motion-corrupted Radon data $\mathcal{R}_{\Gamma}f$ are computed in the 2D parallel scanning geometry with 300 uniformly distributed angles in $[0, 2\pi]$ and 450 detector points.

In Example 22, it is shown that not all singularities of the specimen are ascertained by the measured data. More precisely, a singularity $(x, \xi dx) \in \text{WF}(f)$ is detected if there are $\varphi \in [0, 2\pi]$ and $\sigma \in \mathbb{R}$ such that

$$\xi_0 = \sigma D_x H(\varphi, x) = \sigma \theta \left(\frac{\varphi}{3} \right).$$

Thus,

$$\{\sigma D_x H(\varphi, x) \mid \varphi \in [0, 2\pi], \sigma \in \mathbb{R} \setminus 0\} = \left\{ \sigma \theta(\varphi) \mid \varphi \in \left[0, \frac{2\pi}{3}\right] \cup \left[\frac{4\pi}{3}, 2\pi\right], \sigma \in \mathbb{R} \setminus 0 \right\};$$

i.e., only singularities with direction

$$(45) \quad \xi = \sigma \theta(\varphi_{\xi}), \quad \varphi_{\xi} \in \left[0, \frac{2}{3}\pi\right] \cup \left[\frac{4}{3}\pi, 2\pi\right]$$

are gathered in the data. In other words, singularities with direction $\xi = \sigma \theta(\varphi_{\xi})$, $\varphi_{\xi} \in (\frac{2}{3}\pi, \frac{4}{3}\pi)$ cannot be reconstructed from the dynamic data set.

This is clearly seen in the reconstruction (Figure 2). Here, we used the exact motion functions and the algorithm proposed in [16] as a reconstruction method which compensates

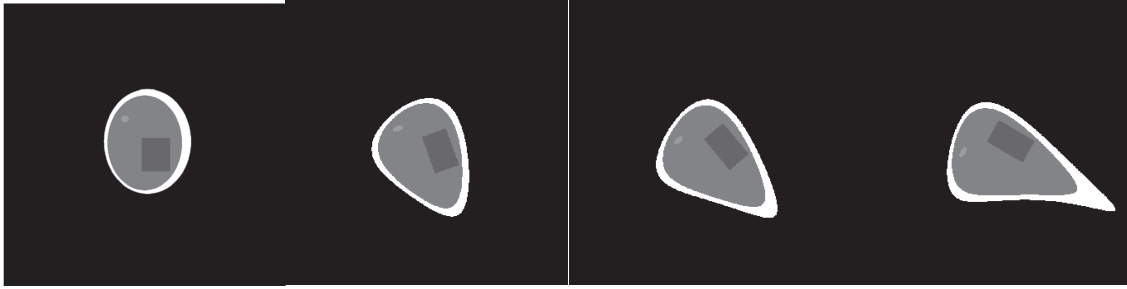


Figure 3. *Nonaffine motion of the phantom during the scanning.*

known affine deformations exactly. The algorithm outlined in [16] is of filtered backprojection type, and hence it fits into our framework of reconstruction operators $\mathcal{L}_{[0,2\pi]} = \mathcal{R}_{\Gamma,\psi}^t \mathcal{P} \mathcal{R}_{\Gamma,[0,2\pi]}$; see (39).

Further, the singularities gathered at time instances $\varphi = 0$ and $\varphi = 2\pi$ create added artifacts along their integration curves. Since

$$C(\varphi, s) = \{x \in \mathbb{R}^2 \mid (\Gamma_\varphi^{-1}x)^T \theta(\varphi) = s\} = \{x \in \mathbb{R}^2 \mid x^T A_\varphi \theta(\varphi) = s\},$$

these added artifacts arise along straight lines with direction $\theta(\frac{4}{3}\pi)^\perp$ and $(\begin{smallmatrix} 0 \\ -1 \end{smallmatrix})$. Thus, the reconstructed image, Figure 2, shows the typical limited angle streak artifacts known from the static case on the angular range $(\frac{2}{3}\pi, \frac{4}{3}\pi)$.

Next, we illustrate our results for a nonaffine motion model, where the integration curves $C(\varphi, s)$ no longer correspond to straight lines. As an example, we consider the nonperiodic motion model

$$\Gamma_\varphi x = \Gamma_\varphi^{\text{scal}} A_\varphi x$$

with rotation matrix

$$A_\varphi = \begin{pmatrix} \cos(\frac{2}{3}\varphi) & \sin(\frac{2}{3}\varphi) \\ -\sin(\frac{2}{3}\varphi) & \cos(\frac{2}{3}\varphi) \end{pmatrix}$$

and

$$\Gamma_\varphi x = \begin{pmatrix} x_1 s_1(\varphi, x) \\ x_2 s_2(\varphi, x) \end{pmatrix}$$

with scaling parameters that depend on the time φ as well as on the particle x ; see [18]. In the numerical example,

$$s_i(\varphi, x) = \sum_{j=0}^4 (\sqrt[4]{5m_i} x_i)^j, \quad i = 1, 2,$$

with $m_1 = \sin(1.5 \cdot 10^{-2} \varphi/\pi)$, $m_2 = \sin(2.1 \cdot 10^{-2} \varphi/\pi)$. The deformation of the object during the data acquisition is illustrated in Figure 3. To compare our reconstruction results, the reference state is shown again in Figure 4.

In [18], a reconstruction method was proposed which compensates for nonaffine motion, and which belongs to the class of reconstruction operators $\mathcal{L}_{[0,2\pi]} = \mathcal{R}_{\Gamma,\psi}^t \mathcal{P} \mathcal{R}_{\Gamma,[0,2\pi]}$; see (39).

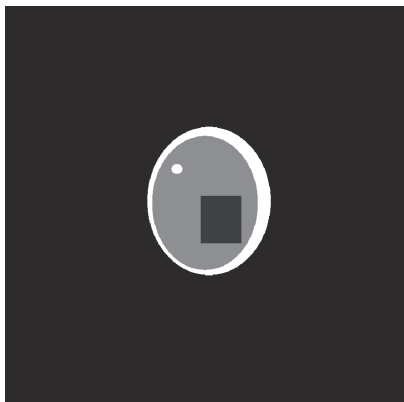


Figure 4. Object in Figure 3 at time instance $t = 0$ (reference object).

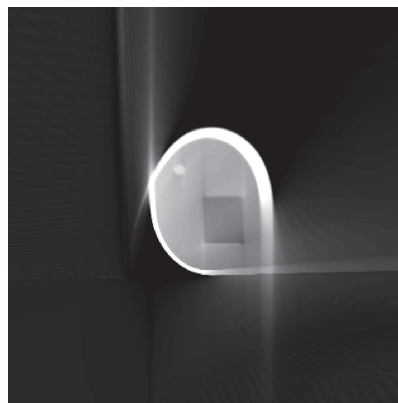


Figure 5. Reconstruction incorporating the exact motion functions of the object in Figure 4.

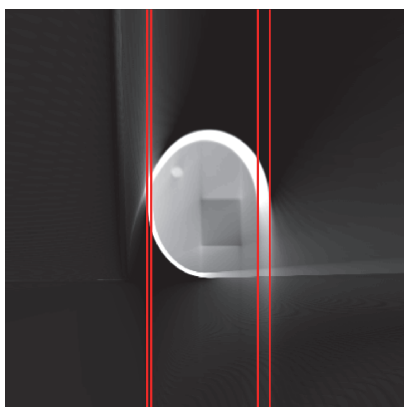


Figure 6. Figure 5 with integration curves tangent to the outer ellipses for $\varphi = 0$ highlighted.

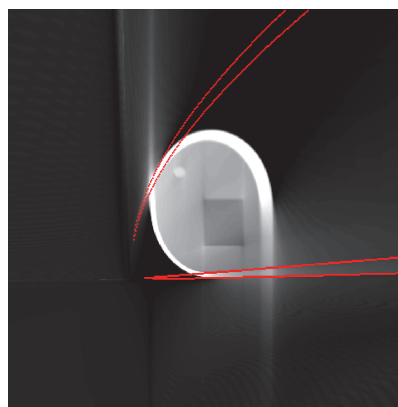


Figure 7. Figure 5 with integration curves tangent to the outer ellipses for $\varphi = 2\pi$ highlighted.

Applying this method to the dynamic data set provides an image showing the visible singularities, i.e., those ascertained in the data, as well as additional artifacts; see Figure 5. Figures 6 and 7 display, in addition, the integration curves passing through the singularities of the two outer ellipses, detected at time instances $\varphi = 0$ and $\varphi = 2\pi$, respectively. The comparison shows that, in agreement with our theory, the additional artifacts spread along these integration curves. Since $\Gamma_0 x = x$, the curves for $\varphi = 0$ are straight lines, whereas at $\varphi = 2\pi$ they are indeed curves, not straight lines.

The artifact reduction strategy described in section 5.3 performs in a way similar to the static case, which has been analyzed in detail, e.g., in [9, 11].

7. Conclusion and outlook. In this article, we showed that the dynamic behavior of the object in computerized tomography can lead to limited data problems, and this means

that certain singularities will be invisible in the reconstruction, regardless of the performance of the motion compensation algorithm. We also provided a characterization of detectable singularities that depends on the exact dynamics, as well as possible added artifacts which arise even if the object’s dynamic behavior is exactly known in the reconstruction step. In applications, this has to be taken into account at the evaluation of the reconstructed images in order to obtain a reliable diagnosis.

Our results can serve as a basis for developing mathematical criteria to distinguish added artifacts arising due to the information content in the data from motion artifacts which occur if the motion is not correctly compensated for. This can have great benefits in applications, for example in the course of estimating the a priori unknown motion parameters which are required in order to apply a motion compensation algorithm for the reconstruction. To this end, one first has to develop a motion model which describes the type of movement performed by the object, and then the parameters of this model have to be estimated from the measured data via analytic [30] or iterative [27] methods. However, the estimated parameters will always be affected by errors, especially in the iterative procedure. Hence, motion artifacts as well as added artifacts described in this article will appear in the reconstructed images. In this case, it is essential to understand and evaluate whether any given artifact is related to an inaccurate motion model and incorrect parameters or whether it is inevitable due to information missing from the data.

Appendix A.

A.1. The forward operator: Proof of Theorem 12. Let $f \in \mathcal{D}(\mathbb{R}^2)$, let \mathcal{F} be the Fourier transform on \mathbb{R}^2 , and let \mathcal{F}_s be the 1D Fourier transform in the s variable with the following normalizations:

$$\mathcal{F}f(\xi) = \frac{1}{2\pi} \int e^{-ix \cdot \xi} f(x) dx, \quad \mathcal{F}_s g(\varphi, \tau) = \frac{1}{\sqrt{2\pi}} \int e^{-i\tau s} g(\varphi, s) ds.$$

Using the *Fourier slice theorem* for the classical Radon line transform with fixed φ ,

$$\mathcal{F}(\mathcal{R}_\Gamma f)(\varphi, \sigma) = \mathcal{F}_s(\mathcal{R}(f \circ \Gamma_\varphi))(\varphi, \sigma) = \sqrt{2\pi} \mathcal{F}(f \circ \Gamma_\varphi)(\sigma\theta(\varphi)).$$

Due to this relation and the substitution $z := \Gamma_\varphi x$, we obtain the following representation:

$$\begin{aligned} \mathcal{R}_\Gamma f(\varphi, s) &= (2\pi)^{-1/2} \int_{\mathbb{R}} e^{i\sigma s} \mathcal{F}_s(\mathcal{R}_\Gamma f)(\varphi, \sigma) d\sigma \\ &= \int_{\mathbb{R}} e^{i\sigma s} \mathcal{F}(f \circ \Gamma_\varphi)(\sigma\theta(\varphi)) d\sigma \\ &= (2\pi)^{-1} \int_{\mathbb{R}} e^{i\sigma s} \int_{\mathbb{R}^2} f(\Gamma_\varphi x) e^{-i\sigma x^T \theta(\varphi)} dx d\sigma \\ &= (2\pi)^{-1} \int_{\mathbb{R}} e^{i\sigma s} \int_{\mathbb{R}^2} f(x) |\det D\Gamma_\varphi^{-1} x| e^{-i\sigma(\Gamma_\varphi^{-1} x)^T \theta(\varphi)} dx d\sigma \\ &= \int_{\mathbb{R}} \int_{\mathbb{R}^2} e^{i\sigma(s - (\Gamma_\varphi^{-1} x)^T \theta(\varphi))} f(x) |\det D\Gamma_\varphi^{-1} x| (2\pi)^{-1} dx d\sigma. \end{aligned}$$

The function

$$\Phi(\varphi, s, x, \sigma) = \sigma(s - (\Gamma_\varphi^{-1}x)^T\theta(\varphi)) = \sigma(s - H(\varphi, x))$$

is homogeneous of degree 1 with respect to σ . A calculation using this definition shows

$$\begin{aligned} \partial_\sigma \Phi &= (s - (\Gamma_\varphi^{-1}x)^T\theta(\varphi)) \, d\sigma = (s - H(\varphi, x)) \, d\sigma, \\ \partial_s \Phi &= \sigma \, ds, \\ \partial_x \Phi &= -\sigma \left((D_x \Gamma_\varphi^{-1}x)^T \right) \theta(\varphi) \, dx = -\sigma \mathcal{N}(\varphi, x) \, dx, \end{aligned}$$

which we justify using (17) and (18). Since Γ_φ is a diffeomorphism, the Jacobian matrix $D_x(\Gamma_\varphi^{-1}x)$ has nowhere-zero determinant, so the product $(D_x(\Gamma_\varphi^{-1}x))^T \theta(\varphi)$ is nowhere zero. Thus, altogether, we obtain that $(\partial_{(\varphi,s)}\Phi, \partial_\sigma\Phi)$ and $(\partial_x\Phi, \partial_\sigma\Phi)$ are nonzero for all (φ, s, x, σ) . Hence, Φ is a phase function. Note that Φ is nondegenerate because $\frac{\partial}{\partial s} \left(\frac{\partial}{\partial \sigma} \Phi \right) = 1$ is nonzero.

Since Γ_φ and its inverse are smooth in (φ, x) , the amplitude of \mathcal{R}_Γ , $a = |D_x(\Gamma_\varphi^{-1}x)|$, and phase function, Φ , are smooth on their respective domains. Furthermore, $a(\varphi, s, x, \sigma)$ does not depend on σ , so it is trivially a symbol of order 0 (see (10)). This means that \mathcal{R}_Γ is an FIO with order $-1/2$. Since Γ_φ is a diffeomorphism for each $\varphi \in (-\epsilon, 2\pi + \epsilon)$, the symbol a is positive and bounded away from zero on every compact set in $(-\epsilon, 2\pi + \epsilon) \times \mathbb{R}^2$ (and arbitrary σ). This shows that the amplitude a is elliptic, and so \mathcal{R}_Γ is an elliptic FIO.

A.2. The forward operator: Proof of Theorem 15. According to Theorem 12, \mathcal{R}_Γ is an FIO. Thus, (26) follows by the Hörmander–Sato lemma (Theorem 8).

Now assume that the motion model in addition fulfills the microlocal Bolker assumption. As noted in Theorem 12, the symbol of \mathcal{R}_Γ is elliptic. The proof of the theorem in full generality follows from the general calculus of FIO in [19], and it will be outlined here.

Let $f \in \mathcal{E}'(\mathbb{R}^2)$, and let $(x_0, \xi_0) \in \text{WF}(f) \cap \mathcal{V}_{(-\epsilon, 2\pi + \epsilon)}$. Then the set

$$\mathcal{C}_{\Gamma, (x_0, \xi_0)} = \Pi_R^{-1} \{ (x_0, \xi_0) \}$$

is nonempty. By the microlocal Bolker assumption, Π_L is an immersion, and so Π_R is also an immersion by [19, Proposition 4.1.3]. Therefore, $\mathcal{C}_{\Gamma, (x_0, \xi_0)}$ is a discrete set in \mathcal{C}_Γ . To better understand this set, we will use the diffeomorphism $c : (-\epsilon, 2\pi + \epsilon) \times \mathbb{R}^2 \times (\mathbb{R} \setminus \mathbf{0}) \rightarrow \mathcal{C}_\Gamma$, given in (24). Let

$$\begin{aligned} \lambda_0 &= c(\varphi_0, x_0, \sigma_0) \\ &= (\varphi_0, H(\varphi_0, x_0), \sigma_0(-\partial_\varphi H(\varphi_0, x_0) + ds), x_0, \sigma_0 \mathcal{N}(\varphi_0, x_0)) \in \mathcal{C}_{\Gamma, (x_0, \xi_0)}. \end{aligned}$$

Note that $\xi_0 = \sigma_0 \mathcal{N}(\varphi_0, x_0)$. Without loss of generality, assume $\sigma_0 > 0$. Let

$$\eta_0 = \sigma_0(-\partial_\varphi H(\varphi_0, x_0) + ds).$$

We now prove that there is a neighborhood U of φ_0 such that λ_0 is the only point in $\mathcal{C}_{\Gamma, (x_0, \xi_0)}$ with $\varphi \in U$. Assume otherwise; then there must be a sequence (φ_j) that converges to φ_0 and another sequence (σ_j) in $\mathbb{R} \setminus \mathbf{0}$ such that $\Pi_R(c(\varphi_j, x_0, \sigma_j)) = (x_0, \xi_0)$. However, a calculation using the definitions of Π_R and c shows that $\sigma_j = \frac{\|\xi_0\|}{\|D_x H(\varphi_j, x_0)\|}$. Therefore $\sigma_j \rightarrow \sigma_0$

and $c(\varphi_j, x_0, \sigma_j) \rightarrow c(\varphi_0, x_0, \sigma_0) = \lambda_0$ in $\mathcal{C}_{\Gamma, (x_0, \xi_0)}$. This contradicts the fact that $\mathcal{C}_{\Gamma, (x_0, \xi_0)}$ is discrete.

Let ϕ_0 be a smooth cutoff function supported in U and equal to one in a smaller neighborhood of φ_0 , and let ϕ_1 be a cutoff function equal to one in a neighborhood of $s_0 = H(\varphi_0, x_0)$. For $(\varphi, s) \in (-\epsilon, 2\pi + \epsilon) \times \mathbb{R}$ let $\phi(\varphi, s) = \phi_0(\varphi)\phi_1(s)$. Now, let

$$(46) \quad M_\phi(g) = \phi g.$$

Then, $M_\phi : \mathcal{D}'((-\epsilon, 2\pi + \epsilon) \times \mathbb{R}) \rightarrow \mathcal{E}'((-\epsilon, 2\pi + \epsilon) \times \mathbb{R})$ is trivially a pseudodifferential operator that has amplitude $\phi(\varphi, s)$ (which is constant in η) and is nonzero and hence elliptic at (φ_0, s_0, η_0) .

Let $\mathcal{R}_\Gamma^* : \mathcal{E}'((-\epsilon, 2\pi + \epsilon) \times \mathbb{R}) \rightarrow \mathcal{D}'(\mathbb{R}^2)$ be the formal adjoint of $\mathcal{R}_\Gamma : \mathcal{D}(\mathbb{R}^2) \rightarrow \mathcal{E}'((-\epsilon, 2\pi + \epsilon) \times \mathbb{R})$. Note that, in this nonperiodic case, \mathcal{R}_Γ^* is not the backprojection defined by (34) but the dual operator defined by (37). Furthermore, \mathcal{R}_Γ^* is an FIO with canonical relation \mathcal{C}_Γ^t .

Because ϕ has compact support, \mathcal{R}_Γ^* , M_ϕ , and \mathcal{R}_Γ can be composed. Because Π_L is an immersion, \mathcal{C}_Γ and \mathcal{C}_Γ^t are local canonical graphs, so the composition $\mathcal{R}_\Gamma^* M_\phi \mathcal{R}_\Gamma$ is an FIO associated with the canonical relation

$$\mathcal{C}_\Gamma^t \circ \mathcal{C}_\Gamma \subset \Delta := \{(x, \xi; x, \xi) \mid (x, \xi) \in T^*(\mathbb{R}^2) \setminus \mathbf{0}\}.$$

Since $\mathcal{C}_\Gamma^t \circ \mathcal{C}_\Gamma \subset \Delta$, $\mathcal{R}_\Gamma^* M_\phi \mathcal{R}_\Gamma$ is a pseudodifferential operator.

The top order symbol of $\mathcal{R}_\Gamma^*(M_\phi \mathcal{R}_\Gamma)$ at (x_0, ξ_0) is essentially

$$(47) \quad \phi(\varphi_0, H(\varphi_0, x_0)) \frac{|\det(D_x \Gamma_{\varphi_0} x_0)|^2}{2\pi \|\xi_0\|},$$

as can be shown using the symbol calculation in the proof of Theorem 2.1 in [35]. Also, as $\Pi_R : \mathcal{C}_\Gamma \rightarrow T^*(\mathbb{R}^2) \setminus \mathbf{0}$ is a conic immersion, the inverse function theorem shows that φ is a smooth function of (x, ξ) , at least for φ near φ_0 and for x near x_0 . We use that this symbol is nonzero on only one element of $\mathcal{C}_{\Gamma, (x_0, \xi_0)}$, λ_0 , since φ_0 is the only angle in U associated to an element of $\mathcal{C}_{\Gamma, (x_0, \xi_0)}$. This symbol is elliptic near (x_0, ξ_0) because it is nonzero and homogeneous in ξ . Therefore, $\mathcal{R}_\Gamma^*(M_\phi \mathcal{R}_\Gamma)$ is elliptic near $(x_0, \xi_0 dx)$. So, as $(x_0, \xi_0 dx) \in \text{WF}(f)$,

$$(x_0, \xi_0) \in \text{WF}(\mathcal{R}_\Gamma^*(M_\phi \mathcal{R}_\Gamma)).$$

Let $\Pi_L^t : \mathcal{C}_\Gamma^t \rightarrow T^*((-\epsilon, 2\pi + \epsilon) \times \mathbb{R})$ and $\Pi_R^t : \mathcal{C}_\Gamma^t \rightarrow T^*(\mathbb{R}^2)$ be the natural projections. Since

$$(x_0, \xi_0 dx) \in \text{WF}(\mathcal{R}_\Gamma^*[M_\phi \mathcal{R}_\Gamma(f)]) \subset \mathcal{C}_\Gamma^t \circ \text{WF}(M_\phi \mathcal{R}_\Gamma f) = \Pi_R^t \left((\Pi_L^t)^{-1} (\text{WF}(M_\phi \mathcal{R}_\Gamma f)) \right),$$

some element of $\Pi_L^t(\mathcal{C}_{\Gamma, (x_0, \xi_0)})$ is in $\text{WF}(M_\phi \mathcal{R}_\Gamma f)$. Since λ_0 is the only covector in $\mathcal{C}_{\Gamma, (x_0, \xi_0)}$ on which the symbol of $\mathcal{R}_\Gamma^* M_\phi \mathcal{R}_\Gamma$ is nonzero, $\Pi_L(\lambda_0) = (\varphi_0, H(\varphi_0, x_0), \eta_0)$ is the only element of $\Pi_L^t(\mathcal{C}_{\Gamma, (x_0, \xi_0)})$ on which M_ϕ is nonzero. Therefore, $(\varphi_0, H(\varphi_0, x_0), \eta_0) \in \text{WF}(\mathcal{R}_\Gamma f)$.

A.3. The smoothly periodic case: Proof of Theorem 24. The proof of the theorem in full generality follows from arguments in [13, 15, 35].

Since the motion model is smoothly periodic, we can use Proposition 23 to infer that $\mathcal{R}_\Gamma : \mathcal{E}'(\mathbb{R}^2) \rightarrow \mathcal{E}'([0, 2\pi] \times \mathbb{R})$ and $\mathcal{R}_\Gamma^t : \mathcal{D}'([0, 2\pi] \times \mathbb{R}) \rightarrow \mathcal{D}'(\mathbb{R}^2)$ (which is the formal adjoint in this case) are both continuous and can be composed with any pseudodifferential operator $\mathcal{P} : \mathcal{E}'([0, 2\pi] \times \mathbb{R}) \rightarrow \mathcal{D}'([0, 2\pi] \times \mathbb{R})$.

We first show

$$(48) \quad \Pi_R : \mathcal{C}_\Gamma \rightarrow T^*(\mathbb{R}^2) \setminus \mathbf{0} \text{ is surjective.}$$

This will imply that

$$\Pi_R (\Pi_L^{-1} (T^*([0, 2\pi] \times \mathbb{R}) \setminus \mathbf{0})) = T^*(\mathbb{R}^2) \setminus \mathbf{0},$$

so, from the discussion in section 3.2, $\mathcal{V}_{[0, 2\pi]} = T^*(\mathbb{R}^2) \setminus \mathbf{0}$, and every singularity is in $\mathcal{V}_{[0, 2\pi]}$ (i.e., visible in the data according to Definition 17).

By (23), $D_x H(\varphi, x)$ is never zero (or the determinant $\text{IC}(x, \varphi)$ would be zero). For the same reason, $D_\varphi (D_x H(\varphi, x))$ is never zero, and $D_x H(\varphi, x)$ and $D_\varphi (D_x H(\varphi, x))$ are not parallel.

Fix $x_0 \in \mathbb{R}^2$. Consider the function $A : [0, 2\pi] \rightarrow S^1$ defined by

$$A(\varphi) := \frac{D_x H(\varphi, x_0)}{\|D_x H(\varphi, x_0)\|} \in S^1.$$

The map A is periodic of period 2π and continuous since the motion model is smoothly periodic. Because $D_x H(\varphi, x_0)$ and $D_\varphi (D_x H(\varphi, x_0))$ are not parallel, a calculus exercise shows that $A'(\varphi)$ is never zero. Therefore, the 2π -periodic path

$$[0, 2\pi] \ni \varphi \mapsto A(\varphi) \in S^1$$

starts at $A(0)$ and ends at $A(2\pi) = A(0)$ and moves in only one direction. This shows that the range of $\varphi \mapsto A(\varphi)$ is all of S^1 .

Let $x_0 \in \mathbb{R}^2$ and $\xi_0 \in \mathbb{R}^2 \setminus \mathbf{0}$. Let $\varphi_0 \in [0, 2\pi]$ be an angle so that $D_x H(\varphi_0, x_0)$ is parallel to ξ_0 . This can be done because $\varphi \mapsto A(\varphi)$ has range S^1 . In the global coordinates on \mathcal{C}_Γ given by (24),

$$(49) \quad \Pi_R (c(\varphi_0, x_0, \sigma)) = (x_0, \sigma \mathcal{N}(\varphi_0, x_0)),$$

and for appropriate $\sigma \neq 0$, $\sigma D_x H(\varphi_0, x_0) = \xi_0$. Therefore $\Pi_R : \mathcal{C}_\Gamma \rightarrow T^*(\mathbb{R}^2) \setminus \mathbf{0}$ is surjective.

Furthermore, because $A'(\varphi)$ is never zero and $[0, 2\pi]$ is compact, there are at most a finite number of angles $\varphi \in [0, 2\pi]$ with $A(\varphi) = \xi_0 / \|\xi_0\|$. This shows that there are only a finite number of points in \mathcal{C}_Γ that map to (x_0, ξ_0) . (Here one can use (49) to show that, for each (φ, x_0) , $\sigma \mapsto \Pi_R (c(\varphi, x_0, \sigma))$ is one-to-one.)

Now, we prove the theorem. Because Π_R is surjective and Π_L is injective, $\mathcal{C}_\Gamma^t \circ \mathcal{C}_\Gamma = \Delta$. Because \mathcal{C}_Γ and \mathcal{C}_Γ^t are local canonical graphs and \mathcal{R}_Γ^* , \mathcal{P} , and \mathcal{R}_Γ can be composed as FIO, the composition

$$\mathcal{L} = \mathcal{R}_\Gamma^* \mathcal{P} \mathcal{R}_\Gamma$$

is a pseudodifferential operator.

We now explain why \mathcal{L} is elliptic. Let $(x_0, \xi_0) \in T^*(\mathbb{R}^2) \setminus \mathbf{0}$. By the discussion about the map A above, there are a finite number of angles $\{\varphi_0, \dots, \varphi_N\}$ such that $\Pi_R(c(\varphi_j, x_0, \sigma_j)) = (x_0, \xi_0)$.

The symbol of \mathcal{R}_Γ at $c(\varphi_j, x_0, \sigma_j)$ is $a = |D_x \Gamma_{\varphi_j} x_0|$ (see (20)), and the symbol of \mathcal{R}_Γ^* is the same [19]. Let p be the symbol of \mathcal{P} . Then, by the calculus of FIO, the top order symbol of \mathcal{L} at (x_0, ξ_0) is the sum of $a^2 p / \|\xi\|$ summed at each element of the finite set

$$(50) \quad S = \{c(\varphi_j, x_0, \sigma_j) \mid j = 0, \dots, N\}.$$

The proof of this statement is completely analogous to the proof of Theorem 2.1 and equation (15) in [35].

Since each term in this finite sum is positive, as the symbol p is everywhere positive and elliptic, the symbol of \mathcal{L} is positive. Therefore, \mathcal{L} is an elliptic pseudodifferential operator. (The complete argument is analogous to the symbol calculation in the proof of Theorem 2.1 in [35].) This proves our theorem.

Remark 29. Looking over the end of the proof of Theorem 24, one sees that the condition for ellipticity is fulfilled as long as the sum of $a^2 p / \|\xi\|$ evaluated at each element of the finite set S given by (50) is an elliptic symbol.

This discussion shows that \mathcal{P} needs to be elliptic only on $\Pi_L(\mathcal{C}_\Gamma)$, since S is the only set at which the symbol is summed, and S is a subset of \mathcal{C}_Γ , so its symbol p is evaluated only on points in $\Pi_L(\mathcal{C}_\Gamma)$. Examples of such pseudodifferential operators are the operator of Lambda tomography, $-d^2/ds^2$, and the standard filtered backprojection filter for the linear Radon line transform, $\sqrt{-d^2/ds^2}$.

A.4. The nonperiodic case: Proofs of Theorems 26 and 28.

Proof of Theorem 26. We apply a paradigm given in [10] that characterizes the visible and added singularities in a broad range of incomplete data tomography problems. The paradigm uses the following result, which is a special case of a result of Hörmander [20].

Lemma 30. *Let $u \in \mathcal{E}'((-\epsilon, 2\pi + \epsilon) \times \mathbb{R})$, and let B be a closed subset of $(-\epsilon, 2\pi + \epsilon) \times \mathbb{R}$ with nontrivial interior. If the following noncancellation condition holds,*

$$(51) \quad \forall (y, \xi) \in \text{WF}(u), \quad (y, -\xi) \notin \text{WF}(\chi_B),$$

then the product $\chi_B u$ can be defined as a distribution. In this case,

$$\text{WF}(\chi_B u) \subset \mathcal{Q}(B, \text{WF}(u)),$$

where for $W \in T^((-\epsilon, 2\pi + \epsilon) \times \mathbb{R})$*

$$(52) \quad \mathcal{Q}(B, W) := \{(y, \xi + \eta) \mid y \in B, [(y, \xi) \in W \text{ or } \xi = 0] \text{ and } [(y, \eta) \in \text{WF}(\chi_B) \text{ or } \eta = 0]\}.$$

To prove Theorem 26, we apply this paradigm to the FIO \mathcal{R}_Γ with the data set $B := [0, 2\pi] \times \mathbb{R}$. We first use this lemma to establish that the operator $\mathcal{L}_{[0, 2\pi]}$ is well defined.

Proposition 31. For $f \in \mathcal{E}'(\mathbb{R}^2)$, $\chi_{[0,2\pi] \times \mathbb{R}}$ can be multiplied by $\mathcal{R}_\Gamma f$ as distributions. Let ψ be a smooth function equal to 1 on $[0, 2\pi]$ and supported in $(-\epsilon, 2\pi + \epsilon)$, and let $\mathcal{R}_{\Gamma, \psi}^t = \mathcal{R}_\Gamma^* \psi$. Then, for \mathcal{P} a pseudodifferential operator, $\mathcal{R}_{\Gamma, \psi}^t$, \mathcal{P} , and $\chi_{[0,2\pi] \times \mathbb{R}} \mathcal{R}_\Gamma$ can all be composed; $\mathcal{L}_{[0,2\pi]}$ given in (39) is defined; and $\mathcal{L}_{[0,2\pi]} : \mathcal{E}'(\mathbb{R}^2) \rightarrow \mathcal{D}'(\mathbb{R}^2)$.

Proof. First, we show that $\mathcal{P} \mathcal{R}_{\Gamma, [0,2\pi]} f$ is a distribution. The product $\chi_{[0,2\pi] \times \mathbb{R}} \mathcal{R}_\Gamma f$ is well defined for distributions $f \in \mathcal{E}'(\mathbb{R}^2)$, since $\text{WF}(\chi_{[0,2\pi] \times \mathbb{R}})$ has ds component of zero, whereas any covector in $\mathcal{C}_\Gamma \circ \text{WF}(f)$ has nonzero ds component by the definition of \mathcal{C}_Γ , (21). Therefore, the noncancellation condition in Lemma 30 holds, and $\chi_{[0,2\pi] \times \mathbb{R}} \mathcal{R}_\Gamma f$ is a distribution.

We claim that $\chi_{[0,2\pi] \times \mathbb{R}} \mathcal{R}_\Gamma f$ has compact support. First, this distribution has support in $[0, 2\pi] \times \mathbb{R}$ because $\chi_{[0,2\pi] \times \mathbb{R}}$ does. Since, for each φ , $s \mapsto C(\varphi, s)$ is a smooth foliation of the plane, for each φ , the support in s of $\chi_{[0,2\pi] \times \mathbb{R}} \mathcal{R}_\Gamma f(\varphi, \cdot)$ is compact. Since the foliation depends smoothly on φ and because φ is in the compact set $[0, 2\pi]$, there is an $M > 0$ such that the support of $\chi_{[0,2\pi] \times \mathbb{R}} \mathcal{R}_\Gamma f$ is in $[0, 2\pi] \times [-M, M]$. Therefore, $\mathcal{P} \mathcal{R}_{\Gamma, [0,2\pi]} f$ is defined as a distribution in $\mathcal{D}'((-\epsilon, 2\pi + \epsilon) \times \mathbb{R})$.

One proves that $\psi \mathcal{R}_\Gamma$ is continuous from $\mathcal{D}(\mathbb{R}^2)$ to $\mathcal{D}'((-\epsilon, 2\pi + \epsilon) \times \mathbb{R})$ using the same arguments as in the proof of Proposition 23. This implies that $(\psi \mathcal{R}_\Gamma)^* = \mathcal{R}_\Gamma^* \psi = \mathcal{R}_{\Gamma, \psi}^t$ is weakly continuous from $\mathcal{D}'((-\epsilon, 2\pi + \epsilon) \times \mathbb{R})$ to $\mathcal{D}'(\mathbb{R}^2)$. Therefore, $\mathcal{L}_{[0,2\pi]} f$ is defined as a distribution. ■

We continue the proof of Theorem 26 and now use Theorem 8 to show

$$(53) \quad \text{WF}(\mathcal{R}_\Gamma f) \subset \mathcal{C}_\Gamma \circ \text{WF}(f).$$

Next, we use Lemma 30 to get an upper bound for $\text{WF}(\mathcal{P} \mathcal{R}_{\Gamma, [0,2\pi]} f)$. Using (52) and (53), we obtain

$$\text{WF}(\mathcal{P} \mathcal{R}_{\Gamma, [0,2\pi]} f) \subset \mathcal{Q}([0, 2\pi] \times \mathbb{R}, \text{WF}(\mathcal{R}_\Gamma f)) \subset \mathcal{Q}([0, 2\pi] \times \mathbb{R}, \mathcal{C}_\Gamma \circ \text{WF}(f)),$$

where

$$\begin{aligned} \mathcal{Q}([0, 2\pi] \times \mathbb{R}, \mathcal{C}_\Gamma \circ \text{WF}(f)) = & [(\mathcal{C}_\Gamma \circ \text{WF}(f)) \cap T_{[0,2\pi] \times \mathbb{R}}^*((-\epsilon, 2\pi + \epsilon) \times \mathbb{R})] \\ & \cup \text{WF}(\chi_{[0,2\pi] \times \mathbb{R}}) \cup W_{\{0,2\pi\}}(f) \end{aligned}$$

and where $T_{[0,2\pi] \times \mathbb{R}}^*((-\epsilon, 2\pi + \epsilon) \times \mathbb{R})$ is defined in (29) and

$$\begin{aligned} W_{\{0,2\pi\}}(f) = & \left\{ (\varphi, s, \sigma ds + [\mu - \sigma \partial_\varphi H(\varphi, x)] d\varphi) \mid \right. \\ & \sigma, \mu \neq 0, \varphi \in \{0, 2\pi\}, s \in \mathbb{R}, \\ & \left. x \in C(\varphi, s), \text{ and } (x, \sigma \mathcal{N}(\varphi, x)) \in \text{WF}(f) \right\}. \end{aligned}$$

Equivalently, this set can be written as

$$(54) \quad W_{\{0,2\pi\}}(f) = \left\{ (\varphi, s, \sigma ds + \nu d\varphi) \mid \sigma \neq 0, \nu \in \mathbb{R}, \varphi \in \{0, 2\pi\}, s \in \mathbb{R}, \right. \\ \left. \exists x \in C(\varphi, s), (x, \sigma \mathcal{N}(\varphi, x)) \in \text{WF}(f) \right\}.$$

To accomplish the final step of the paradigm, we determine

$$\mathcal{C}_\Gamma^t \circ \mathcal{Q}([0, 2\pi] \times \mathbb{R}, \mathcal{C}_\Gamma \circ \text{WF}(f)),$$

which corresponds to computing the three components

$$\begin{aligned} \mathcal{C}_\Gamma^t \circ \mathcal{Q}([0, 2\pi] \times \mathbb{R}, \mathcal{C}_\Gamma \circ \text{WF}(f)) &= \mathcal{C}_\Gamma^t \circ [(\mathcal{C}_\Gamma \circ \text{WF}(f)) \cap T_{[0, 2\pi] \times \mathbb{R}}^*((-\epsilon, 2\pi + \epsilon) \times \mathbb{R})] \\ &\quad \cup \mathcal{C}_\Gamma^t \circ \text{WF}(\chi_{[0, 2\pi] \times \mathbb{R}}) \\ &\quad \cup \mathcal{C}_\Gamma^t \circ W_{\{0, 2\pi\}}(f). \end{aligned}$$

Since \mathcal{C}_Γ fulfills the microlocal Bolker assumption, $\mathcal{C}_\Gamma^t \circ \mathcal{C}_\Gamma \circ \text{WF}(f) \subset \text{WF}(f)$. Thus, for the first component, we obtain

$$\mathcal{C}_\Gamma^t \circ [(\mathcal{C}_\Gamma \circ \text{WF}(f)) \cap T_{[0, 2\pi] \times \mathbb{R}}^*((-\epsilon, 2\pi + \epsilon) \times \mathbb{R})] \subset \text{WF}(f) \cap \mathcal{V}_{[0, 2\pi]},$$

i.e., the set of visible singularities with data from $[0, 2\pi] \times \mathbb{R}$: $\text{WF}_{[0, 2\pi]}(f)$.

For the second component, $\mathcal{C}_\Gamma^t \circ \text{WF}(\chi_{[0, 2\pi] \times \mathbb{R}}) = \emptyset$, since the ds component of any covector in $\text{WF}(\chi_{[0, 2\pi] \times \mathbb{R}})$ is zero and all covectors in \mathcal{C}_Γ^t have nonzero ds component.

Lastly, we consider $\mathcal{C}_\Gamma^t \circ W_{\{0, 2\pi\}}(f)$ and show that this equals the set of additional artifacts $\mathcal{A}(f)$. To this end, we let

$$\rho = (\varphi, s, \nu d\varphi + \sigma ds) \in W_{\{0, 2\pi\}}(f),$$

and so $\varphi \in \{0, 2\pi\}$, $s, \nu \in \mathbb{R}$, $\sigma \neq 0$, and there is an $x \in C(\varphi, s)$ such that $(x, \sigma \mathcal{N}(\varphi, x)) \in \text{WF}(f)$. Using the definition of composition, one sees

$$\mathcal{C}_\Gamma^t \circ \{\rho\} = \{(\tilde{x}, \sigma(\mathcal{N}(\varphi, \tilde{x}))) \mid (\tilde{x}, \sigma \mathcal{N}(\varphi, \tilde{x}), \rho) \in \mathcal{C}_\Gamma^t\}.$$

By the definition of \mathcal{C}_Γ^t , $\tilde{x} \in C(\varphi, s)$; i.e., $s = H(\tilde{x}, \varphi)$ and $-\nu/\sigma = D_\varphi H(\tilde{x}, \varphi)$. Since ν is arbitrary, for any \tilde{x} in $C(\varphi, s)$ there is a corresponding covector in this composition. Therefore, for any $\tilde{x} \in C(\varphi, s)$, the covector $(\tilde{x}, \sigma \mathcal{N}(\varphi, \tilde{x})) \in \mathcal{C}_\Gamma^t \circ W_{\{0, 2\pi\}}(f)$. Thus, this set corresponds to the set of possible added singularities (41). ■

Proof of Theorem 28. Let $(x_0, \xi_0) \in \mathcal{V}_{(0, 2\pi)}$; then by the uniqueness assumption (42), there is a unique $(\varphi_0, s_0) \in (-\epsilon, 2\pi + \epsilon) \times \mathbb{R}$ such that ξ_0 is conormal to $C(\varphi_0, x_0)$ at x_0 . Since φ_0 is unique and $(x_0, \xi_0) \in \mathcal{V}_{(0, 2\pi)}$, $\varphi_0 \in (0, 2\pi)$. Let σ_0 be the unique nonzero number such that $\xi_0 = \sigma_0 \mathcal{N}(\varphi_0, x_0)$. Then,

$$(55) \quad \lambda_0 = c(\varphi_0, x_0, \sigma_0) \in \mathcal{C}_\Gamma$$

is the unique covector in \mathcal{C}_Γ such that $\Pi_R(\lambda_0) = (x_0, \xi_0)$ (where c is given by (24)). Let

$$(56) \quad \rho_0 := \Pi_L(\lambda_0) = (\varphi_0, s_0, \sigma_0(-\partial_\varphi H(\varphi_0, x_0) + ds)).$$

We note that

$$(57) \quad \{\rho_0\} = \mathcal{C}_\Gamma \circ \{(x_0, \xi_0)\}, \quad \{(x_0, \xi_0)\} = \mathcal{C}_\Gamma^t \circ \{\rho_0\}.$$

These equalities are true by (16) and the microlocal Bolker assumption because λ_0 is the only element in $\Pi_R^{-1}\{(x_0, \xi_0)\}$.

First, we show $\text{WF}_{(0,2\pi)}(\mathcal{L}_{[0,2\pi]}f) \subset \text{WF}_{(0,2\pi)}(f)$. Assume the covector

$$(x_0, \xi_0) \in \text{WF}_{(0,2\pi)}(\mathcal{L}_{[0,2\pi]}f).$$

Using the result of the last paragraph, let $\varphi_0 \in (0, 2\pi)$ and $\sigma_0 \neq 0$ be the unique numbers so that $\xi_0 = \sigma_0 \mathcal{N}(\varphi_0, x_0)$. By Theorem 26—in particular, (41)—

$$(x_0, \xi_0) \in \text{WF}_{[0,2\pi]}(f) \cup \mathcal{A}(f).$$

However, $\mathcal{A}(f)$ includes singularities $(x, \sigma \mathcal{N}(\varphi, x))$ only for $\varphi = 0$ or $\varphi = 2\pi$, and by the uniqueness assumption (42), since $\xi_0 = \sigma_0 \mathcal{N}(\varphi_0, x_0)$ and $\varphi_0 \notin \{0, 2\pi\}$, $(x_0, \xi_0) \notin \mathcal{A}(f)$, so $(x_0, \xi_0) \in \text{WF}_{(0,2\pi)}(f)$.

Now, let $(x_0, \xi_0) \in \text{WF}_{(0,2\pi)}(f)$. Ellipticity and the uniqueness assumption will be used to show that $(x_0, \xi_0) \in \text{WF}_{(0,2\pi)}(\mathcal{L}_{[0,2\pi]}f)$. Let $\varphi_0, s_0, \sigma_0, \lambda_0$, and ρ_0 be as in the first paragraph of this proof for (x_0, ξ_0) . As noted above, $\varphi_0 \in (0, 2\pi)$ by the uniqueness assumption. Let M_ϕ be the cutoff operator given by (46) in the proof of Theorem 15. The function ϕ in the definition of M_ϕ is the product of two compactly supported cutoff functions, $\phi_0(\varphi)$ and $\phi_1(s)$, and we assume that the cutoff function at φ_0, ϕ_0 , is also supported in $(0, 2\pi)$. As in the proof of Theorem 15,

$$\mathcal{R}_{\Gamma, \psi}^t \mathcal{P} M_\phi \mathcal{R}_{\Gamma, [0, 2\pi]} = \mathcal{R}_\Gamma^* (\psi \mathcal{P} M_\phi \chi_{[0, 2\pi] \times \mathbb{R}} \mathcal{R}_\Gamma)$$

is an elliptic pseudodifferential operator near (x_0, ξ_0) because its symbol is

$$(58) \quad \phi(\varphi_0, H(\varphi_0, x_0)) p(\rho_0) \frac{|\det(D_x \Gamma_{\varphi_0} x_0)|^2}{2\pi \|\xi_0\|},$$

where p is the top order symbol of \mathcal{P} . (Note that $M_\phi \chi_{[0, 2\pi] \times \mathbb{R}} = M_\phi$ since the support of ϕ is in $(0, 2\pi) \times \mathbb{R}$. Also, the cutoff ψ has no effect on the top order symbol (58) since $\phi \cdot \psi = \phi$, as ψ is equal to one in $[0, 2\pi]$.) So

$$(59) \quad (x_0, \xi_0) \in \text{WF}_{(0,2\pi)}(\mathcal{R}_{\Gamma, \psi}^t \mathcal{P} M_\phi \mathcal{R}_{\Gamma, [0, 2\pi]} f).$$

We now show that

$$(60) \quad (x_0, \xi_0) \notin \text{WF}_{(0,2\pi)}(\mathcal{R}_{\Gamma, \psi}^t (\mathcal{P} M_{(1-\phi)} \chi_{[0, 2\pi] \times \mathbb{R}} \mathcal{R}_\Gamma f))$$

by showing

$$(61) \quad (x_0, \xi_0) \notin \mathcal{C}_\Gamma^t \circ \text{WF}(\mathcal{P} M_{(1-\phi)} \chi_{[0, 2\pi] \times \mathbb{R}} \mathcal{R}_\Gamma f)$$

and then using the Hörmander–Sato lemma, Theorem 8.

Because $(1 - \phi)$ is zero near φ_0 , $M_{(1-\phi)} \mathcal{R}_{\Gamma, [0, 2\pi]} f$ is microlocally smooth near ρ_0 . So, $\psi \mathcal{P} M_{(1-\phi)} \mathcal{R}_{\Gamma, [0, 2\pi]} f$ is microlocally smooth near ρ_0 . But, by (57), ρ_0 is the only covector in $\Pi_L(\mathcal{C}_\Gamma)$ that could map to (x_0, ξ_0) under $\Pi_R^t \circ \Pi_L^t$. Therefore, (61) holds, and this proves (60).

Putting (59) and (60) together, we see that $(x_0, \xi_0) \in \text{WF}(\mathcal{L}_{[0, 2\pi]} f)$, and this finishes the proof. ■

A.5. Our theorems for arbitrary smooth weights. Finally, we explain why our theorems are true even if the weight $|\det D\Gamma_\varphi^{-1}x|$ in the definition of \mathcal{R}_Γ , (7), and the definition of \mathcal{R}_Γ^t , (34), are replaced by smooth positive weights. Basically, this is true because elliptic FIOs associated to the same canonical relation have the same microlocal properties, and Radon transforms that integrate over the same sets (associated to the same double fibration [35, Definition 1.1]) are FIOs with the same canonical relations.

Let μ be a smooth positive function on $(-\epsilon, 2\pi + \epsilon) \times \mathbb{R}^2$; then

$$\mathcal{R}_{\Gamma\mu}f(\varphi, s) = \int_{x \in C(\varphi, s)} f(x)\mu(\varphi, x)dx$$

is an elliptic FIO associated to \mathcal{C}_Γ . This is true by the general theory of Radon transforms as FIOs [13, 15] (see also [35]) because this transform integrates over the same sets, $C(\varphi, s)$, as \mathcal{R}_Γ , and the weight is smooth and nowhere zero.

In the smoothly periodic case, the weight μ for $\mathcal{R}_{\Gamma\mu}$ must be 2π -periodic. In this case, a generalized backprojection can be defined as

$$\mathcal{R}_{\Gamma\nu}^\dagger g(x) = \int_{\varphi \in [0, 2\pi]} g(\varphi, H(\varphi, x))\nu(\varphi, x)d\varphi,$$

where ν is a positive smooth 2π -periodic function. Because the weights are smooth and positive, $\mathcal{R}_{\Gamma\mu}$ and $\mathcal{R}_{\Gamma\nu}^\dagger$ are elliptic and associated to \mathcal{C}_Γ and \mathcal{C}_Γ^t , respectively. The proof of Proposition 23 for $\mathcal{R}_{\Gamma\nu}^\dagger \mathcal{P}\mathcal{R}_{\Gamma\mu}$ does not change, and the other proofs for the smoothly periodic case rest on the fact that these transforms are elliptic and associated with the same canonical relations as \mathcal{R}_Γ and \mathcal{R}_Γ^t .

For the nonperiodic case, the weighted backprojection operator is

$$\mathcal{R}_{\Gamma\phi, \psi, \nu}^t = \int_{\varphi \in (-\epsilon, 2\pi + \epsilon)} \phi(\varphi)\nu(\varphi, x)g(\varphi, H(\varphi, x))d\varphi,$$

where ϕ is a smooth function equal to one on $[0, 2\pi]$ and supported in $(-\epsilon, 2\pi + \epsilon)$. In this case, too, the proofs are the same because the transforms have the same microlocal properties.

Acknowledgments. The first author thanks Tufts University for its hospitality during her stay as a visiting scholar. The second author thanks Saarland University for its hospitality during many visits over the years. The second author is indebted to Jan Boman and Jürgen Frikel for stimulating conversations related to microlocal analysis and tomography, to Alexander Katsevich for insightful comments about this article and the general problem, and to Linh Nguyen for useful comments. The referees’ insightful comments have improved the article, and we thank them also for their effort.

REFERENCES

[1] L. L. BARANNYK, J. FRIKEL, AND L. V. NGUYEN, *On artifacts in limited data spherical radon transform: Curved observation surface*, Inverse Problems, 32 (2016), 015012.
 [2] G. BEYLKIN, *The inversion problem and applications of the generalized Radon transform*, Comm. Pure Appl. Math., 37 (1984), pp. 579–599.

- [3] C. BLONDEL, R. VAILLANT, G. MALANDAIN, AND N. AYACHE, *3d tomographic reconstruction of coronary arteries using a precomputed 4d motion field*, Phys. Med. Biol., 49 (2004), pp. 2197–2208.
- [4] C. R. CRAWFORD, K. F. KING, C. J. RITCHIE, AND J. D. GODWIN, *Respiratory compensation in projection imaging using a magnification and displacement model*, IEEE Trans. Med. Imaging, 15 (1996), pp. 327–332.
- [5] M. DEHOOP, *Microlocal analysis of seismic imaging*, in Inside-Out: Inverse Problems and Applications, G. Uhlmann, ed., Math. Sci. Res. Inst. Publ. 47, Cambridge University Press, Cambridge, UK, 2003, pp. 219–296.
- [6] L. DESBAT, S. ROUX, AND P. GRANGEAT, *Compensation of some time dependent deformations in tomography*, IEEE Trans. Med. Imaging, 26 (2007), pp. 261–269.
- [7] D. V. FINCH, I.-R. LAN, AND G. UHLMANN, *Microlocal analysis of the restricted X-ray transform with sources on a curve*, in Inside Out: Inverse Problems and Applications, G. Uhlmann, ed., Math. Sci. Res. Inst. Publ. 47, Cambridge University Press, Cambridge, UK, 2003, pp. 193–218.
- [8] B. FRIGYIK, P. STEFANOV, AND G. UHLMANN, *The X-ray transform for a generic family of curves and weights*, J. Geom. Anal., 18 (2008), pp. 81–97.
- [9] J. FRIKEL AND E. T. QUINTO, *Characterization and reduction of artifacts in limited angle tomography*, Inverse Problems, 29 (2013), 125007.
- [10] J. FRIKEL AND E. T. QUINTO, *Artifacts in incomplete data tomography with applications to photoacoustic tomography and sonar*, SIAM J. Appl. Math., 75 (2015), pp. 703–725.
- [11] J. FRIKEL AND E. T. QUINTO, *Limited data problems for the generalized Radon transform in \mathbb{R}^n* , SIAM J. Math. Anal., 48 (2016), pp. 2301–2318.
- [12] A. GREENLEAF AND G. UHLMANN, *Non-local inversion formulas for the X-ray transform*, Duke Math. J., 58 (1989), pp. 205–240.
- [13] V. GUILLEMIN, *Some Remarks on Integral Geometry*, technical report, Department of Mathematics, MIT, Cambridge, MA, 1975.
- [14] V. GUILLEMIN, *On some results of Gelfand in integral geometry*, Proc. Sympos. Pure Math., 43 (1985), pp. 149–155.
- [15] V. GUILLEMIN AND S. STERNBERG, *Geometric Asymptotics*, American Mathematical Society, Providence, RI, 1977.
- [16] B. HAHN, *Reconstruction of dynamic objects with affine deformations in dynamic computerized tomography*, J. Inverse Ill-Posed Probl., 22 (2014), pp. 323–339.
- [17] B. N. HAHN, *Null space and resolution in dynamic computerized tomography*, Inverse Problems, 32 (2016), 025006.
- [18] B. N. HAHN, *Efficient algorithms for linear dynamic inverse problems with known motion*, Inverse Problems, 30 (2014), 035008.
- [19] L. HÖRMANDER, *Fourier integral operators*, I, Acta Math., 127 (1971), pp. 79–183.
- [20] L. HÖRMANDER, *The Analysis of Linear Partial Differential Operators. I Distribution Theory and Fourier Analysis*, Classics Math., Springer-Verlag, Berlin, 2003.
- [21] A. A. ISOLA, A. ZIEGLER, T. KOEHLER, W. J. NIESEN, AND M. GRASS, *Motion-compensated iterative cone-beam CT image reconstruction with adapted blobs as basis functions*, Phys. Med. Biol., 53 (2008), pp. 6777–6797.
- [22] A. KATSEVICH, *Local tomography for the limited-angle problem*, J. Math. Anal. Appl., 213 (1997), pp. 160–182.
- [23] A. KATSEVICH, *Improved cone beam local tomography*, Inverse Problems, 22 (2006), pp. 627–643.
- [24] A. KATSEVICH, *Motion compensated local tomography*, Inverse Problems, 24 (2008), 045012.
- [25] A. KATSEVICH, *An accurate approximate algorithm for motion compensation in two-dimensional tomography*, Inverse Problems, 26 (2010), 065007.
- [26] A. KATSEVICH, *Reconstruction algorithms for a class of restricted ray transforms without added singularities*, J. Fourier Anal. Appl., (2016), doi:10.1007/s00041-016-9473-y.
- [27] A. KATSEVICH, M. SILVER, AND A. ZAMYATIN, *Local tomography and the motion estimation problem*, SIAM J. Imaging Sci., 4 (2011), pp. 200–219.
- [28] V. P. KRISHNAN AND E. T. QUINTO, *Microlocal analysis in tomography*, in Handbook of Mathematical Methods in Imaging, 2nd ed., Otmar Scherzer, ed., Springer-Verlag, Berlin, 2015, pp. 847–902.

- [29] P. KUCHMENT, K. LANCASTER, AND L. MOGILEVSKAYA, *On local tomography*, Inverse Problems, 11 (1995), pp. 571–589.
- [30] W. LU AND T. R. MACKIE, *Tomographic motion detection and correction directly in sinogram space*, Phys. Med. Biol., 47 (2002), pp. 1267–1284.
- [31] F. NATTERER, *The Mathematics of Computerized Tomography*, B. G. Teubner, Stuttgart, 1986.
- [32] L. V. NGUYEN, *How strong are streak artifacts in limited angle computed tomography?*, Inverse Problems, 31 (2015), 055003.
- [33] L. V. NGUYEN, *On artifacts in limited data spherical Radon transform: Flat observation surfaces*, SIAM J. Math. Anal., 47 (2015), pp. 2984–3004.
- [34] C. J. NOLAN AND M. CHENEY, *Synthetic aperture inversion*, Inverse Problems, 18 (2002), pp. 221–235.
- [35] E. T. QUINTO, *The dependence of the generalized Radon transform on defining measures*, Trans. Amer. Math. Soc., 257 (1980), pp. 331–346.
- [36] E. T. QUINTO, *Singularities of the X-ray transform and limited data tomography in \mathbb{R}^2 and \mathbb{R}^3* , SIAM J. Math. Anal., 24 (1993), pp. 1215–1225.
- [37] E. T. QUINTO, A. RIEDER, AND T. SCHUSTER, *Local inversion of the sonar transform regularized by the approximate inverse*, Inverse Problems, 27 (2011), 035006.
- [38] E. T. QUINTO AND H. RULLGÅRD, *Local singularity reconstruction from integrals over curves in \mathbb{R}^3* , Inverse Probl. Imaging, 7 (2013), pp. 585–609.
- [39] S. ROUX, L. DESBAT, A. KOENIG, AND P. GRANGEAT, *Exact reconstruction in 2d dynamic CT: Compensation of time-dependent affine deformations*, Phys. Med. Biol., 49 (2004), pp. 2169–2182.
- [40] W. RUDIN, *Functional Analysis*, McGraw-Hill Ser. Higher Math., McGraw-Hill, New York, 1973.
- [41] U. SCHMITT, A. K. LOUIS, C. WOLTERS, AND M. VAUHKONEN, *Efficient algorithms for the regularization of dynamic inverse problems: II. Applications*, Inverse Problems, 18 (2002), pp. 659–676.
- [42] L. SHEPP, S. HILAL, AND R. SCHULZ, *The tuning fork artifact in computerized tomography*, Comput. Graphics Image Process., 10 (1979), pp. 246–255.
- [43] R. D. TARver, D. J. CONCES, AND J. D. GODWIN, *Motion artifacts on CT simulate bronchiectasis*, Amer. J. Roentgenol., 151 (1988), pp. 1117–1119.
- [44] F. TRÈVES, *Introduction to Pseudodifferential and Fourier Integral Operators, Volume 1: Pseudodifferential Operators*, Plenum Press, New York, 1980.
- [45] F. TRÈVES, *Introduction to Pseudodifferential and Fourier Integral Operators, Volume 2: Fourier Integral Operators*, Plenum Press, New York, 1980.